THE ROLE OF INTERNAL CONVECTION IN RESPIRATORY GAS TRANSFER IN LARVAL ZEBRAFISH

Malcolm Hughes

Thesis submitted to the

Faculty of Graduate and Postdoctoral Research

University of Ottawa

In partial fulfillment of the requirements for the

MSc Degree in Biology

Department of Biology

Faculty of Science

University of Ottawa

© Malcolm Hughes, Ottawa, Canada, 2018

ABSTRACT

Purely diffusive O_2 transport typically is insufficient to sustain aerobic metabolism in most multicellular organisms. In small animals, however, a high surface-to-volume ratio may allow passive diffusion alone to supply sufficient O_2 transfer. The purpose of this thesis was to explore the impacts of internal convection on the exchange of respiratory gases in a small complex organism, the larval zebrafish (*Danio rerio*). Thus, I tested the hypothesis that internal convection is required for the normal transfer of the respiratory gases O_2 and CO_2 and maintenance of resting aerobic metabolic rate. Use of morpholino knockdown of the VEGF-A and TNNT2 proteins allowed examination of two independent models lacking internal convection. Using micro-respirometry, I demonstrated that loss of internal convection reduces resting rates of O_2 consumption and CO_2 excretion in larvae at 4 days post fertilization. I also used the scanning micro-optrode technique to demonstrate that acute loss of internal convection resulted in reduced rates of cutaneous O_2 flux, a trait that was reversed upon the restoration of internal convection. Finally, I demonstrated that in larval zebrafish, loss of internal convection resulted in decreased hypoxic performance and loss or severe reduction of the hypoxic cardiorespiratory responses. The results from these experiments showed that internal convection is i) required to maintain resting rates of respiratory gas transfer in the larval zebrafish, ii) important in facilitating the hypoxic cardiorespiratory responses in larval zebrafish and iii) augments O_2 extraction capacity in the face of progressive hypoxia.

RÉSUMÉ

Le transport d'O_2 purement diffusif est typiquement insuffisant pour maintenir le métabolisme aérobie dans la plupart des organismes multicellulaires. Dans les petits animaux, cependant, un rapport surface-volume élevé peut permettre à la diffusion passive seule d'etre suffissante pour fournir un transfert d'O_2 suffisant. Le but de cette thèse était d'explorer les impacts de la convection interne sur l'échange des gaz respiratoires dans un petit organisme complexe, le poisson zèbre larvaire (*Danio rerio*). Ainsi, j'ai testé l'hypothèse que la convection interne est nécessaire pour le transfert normal des gaz respiratoires O_2 et CO_2 et le maintien du taux métabolique aérobie au repos chez le poisson zèbre larvaire. L'utilisation du knock-out morpholino des protéines VEGF-A et TNNT2 a permis d'examener deux modèles indépendants dépourvus de convection interne. En utilisant la micro-respirométrie, j'ai démontré que la perte de convection interne réduit les taux au repos de la consommation d'O_2 et l'excrétion de CO_2 chez les larves de poisson zèbre 4 jours après la fécondation. J'ai également utilisé la technique de micro-optrode de balayage pour démontrer que la perte aiguë de convection interne entraînait des taux réduits de flux cutané d'O_2, un caractère qui était inversé lors de la restauration de la convection interne. Enfin, j'ai démontré que chez les larves de poisson-zèbre, la perte de convection interne a entraîné une diminution de la performance hypoxique et de la perte ou une réduction sévère des réponses cardiorespiratoires hypoxiques. Les résultats de ces expériences ont demontré que la convection interne est necessaire i) pour maintenir les taux de transfert des gaz respiratoires chez les larves de poisson zèbre, ii) est importante pour faciliter les réponses cardiorespiratoires hypoxiques chez le poisson zèbre larvaire et iii) augmente la capacité d'extraction d'O_2 face à une hypoxie progressive.

Acknowledgments

First and foremost, I'd like to thank Dr. Steve Perry for granting me the opportunity to work and learn in his lab. Under his supervision throughout the years, I've not only learned how to be a more competent researcher, but I also learned about myself and as such grew as an individual. Steve gave me great freedom to explore and learn on my own, but was always there to provide counsel and guidance when needed. His oversight shaped my masters' thesis and was irrefutably essential to its success. Working with Dr. Perry over the course of my degree has been an unforgettable experience and the skills I've acquired will carry with me wherever I go in the future.

I'd like to thank Drs. Katie Gilmour, Tom Moon and Steve Cooke for their insightful comments, constructive criticism and sound suggestions. I've benefited a great deal from their input on my work.

I'd like to thank all of the members of the Perry and Gilmour labs, both past and present, for the innumerable myriad of favours, advice and general comradery that really distinguished the lab and always made me feel right at home. This group managed to make the inherent challenges of research a little bit easier and a lot more fun. As spectacular as the whole group is overall, I'd like to give a special thanks to two particular individuals: Drs. Alex Zimmer and Milica Mandic.

Dr. Alex Zimmer was a key resource in helping me work through the perplexities of the SMOT technique. From troubleshooting results to experimental design, without his help I wouldn't have achieved several critical experiments central to my thesis. Furthermore, his jovial

nature and open-mindedness made working with him exceptionally easy and enjoyable. Dr. Milica Mandic has been invaluable in helping me interpret, piece together and generally complete my thesis. Her incredible patience (even in the face of my often woeful ignorance), coupled with her veritable wealth of statistical and physiological knowledge, has been stupendously helpful throughout my journey. I am extremely fortunate to have had all of the help and guidance provided by both of these individuals, without whom this thesis would bear scant resemblance to what it is today.

I'd like to say a thanks to all of the aquatics staff at the University of Ottawa for ensuring that I had the animals I needed, how and when I needed them, with a special thanks to Bill Fletcher, Christine Archer and Vishal Saxena. Lastly, I'd like to thank my friends and family for their continued and steadfast support, especially my partner Sofia, who's understanding, encouragement and overall assistance has been pivotal to the completion and general success of my masters.

TABLE OF CONTENTS

LIST OF FIGURES

LIST OF TABLES

LIST OF ABBREVIATIONS

ANOVA, analysis of variance

CO_2, carbon dioxide

DAPI, 4',6-diamidino-2-phenylindole

Dpf, days post fertilization

f_H, cardiac frequency

f_v, ventilation frequency

g, gram

h, hour

Hb, hemoglobin

HCl, hydrochloric acid

Hpf, hours post fertilization

JO_2, O_2 flux rate

KOH, potassium hydroxide

L, liter

M, molar

$\dot{M}CO_2$, rate of carbon dioxide excretion

MeOH, methanol

min, minutes

ml, milliliter

mm, millimeter

mM, millimolar

$\dot{M}O_2$, rate of oxygen production

MS-222, tricaine methanesulfonate

nl, nanoliter

O_2, oxygen

PBS, phosphate-buffered saline

PBST, phosphate-buffered saline solution with tween

tween, polysorbate

P_{crit}, critical partial pressure of O_2

PFA, paraformaldehyde

pH, potential of hydrogen

PO_2, partial pressure of O_2

Pt-TFPP, Pt(II) meso-Tetra(pentaflourophenyl)porphyrin

RER, respiratory exchange ratio

rpm, revolutions per minute

s, seconds

SEM, standard error of the mean

SMOT, scanning micro optrode technique

V, volume

WT, wild type

µl, microliter

µm, micrometer

µM, micromolar

CHAPTER 1

General Introduction

1.1 INTRODUCTION

"*The world belongs to the energetic*" ***Ralph Waldo Emerson***

All living organisms require energy to survive. Much like a fire requires oxygen (O_2) to burn, O_2 is necessary for most living organisms to sustain the aptly coined 'fire of life' (Kleiber, 1961). Most higher vertebrates rely heavily on O_2 to meet their energetic needs through aerobic metabolism. When a fuel source, for example glucose, transfers electrons to another molecule, the glucose is said to be oxidized. This oxidation process releases energy as the electrons are transferred. Most enzymes however, are not equipped to harness this available energy and therefore the energy is converted to adenosine tri-phosphate (ATP). ATP molecules are the energetic currency of the cell and contain high-energy phosphate bonds that store the energy released from oxidation in a form that is more readily utilized within the cell.

Energy can be produced in the absence of O_2 and when this occurs, it is known as anaerobic respiration. Anaerobic respiration occurs when a molecule other than O_2 is used as the final acceptor of the electrons, such as lactate during glycolysis. Anaerobic glycolysis is significantly less efficient than aerobic respiration. For example, for a single molecule of glucose, using O_2-based aerobic metabolism and the mitochondrial enzymatic machinery produces ~30 ATP. Utilizing the same molecule of glucose for anaerobic metabolism produces only 2 ATP, thus aerobic respiration is approximately 15 times more efficient than anaerobic

metabolism (Rich, 2003). Aerobic respiration also greatly improves the variety of potential fuel sources to include not only carbohydrates but also lipids and proteins (Kleiber, 1961).

Aerobic energy production occurs through the process of oxidative phosphorylation. Oxidative phosphorylation relies upon two key steps that occur after glycolysis, both of which occur inside the mitochondria (Weibel, 1984). The first is the citric acid (or Kreb's) cycle in which reduced compounds, namely NADH and $FADH_2$ are formed in addition to some ATP. The second step lies in the electron transport chain where these reduced compounds are harnessed to drive a proton gradient that powers the enzyme complex ATP synthase that generates the majority of the ATP produced by aerobic respiration. Both the citric acid cycle and the electron transport chain require O_2 as the terminal electron acceptors at various steps along the pathway. As the mitochondria perform aerobic respiration, they consume the O_2 through the Krebs cycle and the electron transport chain, where it is transformed into CO_2 and water (Rich, 2003). This removal of O_2 ultimately makes mitochondria the O_2 sink, or the final destination for cellular O_2.

1.2 Movement of O_2

The O_2 consumed by mitochondria ultimately must be replaced for aerobic respiration to continue. There are two ways this can occur, the first is through simple diffusion. Diffusion operates based on the principle that gases move according to partial pressure gradients from the area of highest partial pressure towards the area of lowest partial pressure, until equilibrium is attained. The rate at which a molecule diffuses depends on three main factors.

The first is the size of the gradient, the larger the gradient the faster diffusion will occur. The second factor is the resistance of the medium, for example O_2 diffuses 10,000 times faster through air than through water because water has a much higher resistance than air (Richard, 1996a, 1996b; Weibel, 1984). The final factor is temperature, with increasing temperatures raising the kinetic energy of the molecules and ultimately speeding up diffusion, while lower temperatures do the opposite.

The second method for the replenishment of O_2 is convection or mass transport. In convection, the medium containing the substance of interest is moved from location A to location B. This contrasts with simple diffusion where the substance moves *through* the medium. Examples of respiratory convection are tidal pulmonary air flow and unidirectional water flow over their gills. In complex organisms, the net movement of O_2 from the environment to mitochondria is accomplished by the additive effects of diffusion and convection (Perry & Gilmour, 2010).

The ease with which a gas diffuses across a membrane or epithelial barrier is determined by its conductance which, in turn, is affected by the thickness of the barrier, its surface area and its permeability. The diffusion of O_2 across a permeable barrier is inversely proportional to its thickness and directly proportional to surface area and permeability. The permeability for specific gases is represented by a calculated constant referred to as the permeation coefficient (K_x). These relationships can be described by Fick's diffusion equation:

$$\dot{V}O_2\ (A\text{-}B) = K_x \times (S/T) \times [PO_2(A) - PO_2(B)]$$

Where $\dot{V}O_2$ is the rate of movement of O_2 between two locations, 'A' and 'B'. K_x is Krogh's permeation coefficient for the barrier in question, 'S' represents the total surface area of the barrier, T represents the thickness of the barrier and PO_2 represents the partial pressure of O_2 at the given location. Krogh's permeation constant K_x can defined as:

$$K_x = DO_2 \times \beta O_2$$

Where DO_2 represents the diffusion coefficient and βO_2 represents the capacitance coefficient for O_2 in a given medium at any given temperature. Although there are several advantages to an aquatic lifestyle, one significant drawback is the limitation on O_2 availability. As mentioned above, O_2 diffuses 10,000 times more easily through air compared to water. This O_2 challenge is further exacerbated by the fact that water exhibits a 30-fold lower O_2 solubility relative to air (Weibel, 1984). Thus, at equivalent partial pressures, an equal volume of water contains significantly fewer O_2 molecules than air.

When organisms are relatively small they have a comparatively high surface area-to-volume ratio which favors simple diffusion because the distances required for respiratory gases to diffuse are low relative to the high surface areas across which gas diffusion is occurring. As organisms increase in size however, their internal volume increases to a greater extent than their overall surface area, at a rate of about 2:3 for the surface area:internal volume of a sphere. The decrease in surface-to-volume ratio which occurs as organisms increase in size places constraints on simple diffusion alone, to meet the requirements of O_2 delivery to mitochondria (and removal of CO_2). Thus, as organisms increase in size, a point is reached where simple diffusion can no longer satisfy the metabolic requirements. In simple eukaryotes

the size where simple diffusion of O_2 starts to become limiting is about 1 mm (Krogh, 1941). This number is dependant upon the energetic demands of a given organism. As organisms increase in complexity, their energetic demands also tend to increase. Increased complexity also involves more membranes and other less permeable barriers that O_2 must cross to reach the center of the organism, further constraining diffusion as the sole mechanism of O_2 delivery (Chow et al., 2001a; Ferrell & Himmelblau, 1967; Subczynski et al., 1989).

Once an organism exceeds the maximum size where metabolism can be met by simple diffusion, without additional O_2 delivery strategies, an O_2 deficit will develop at the core of the organism. Although anaerobic metabolism could still occur and contribute to the net energy supply, it is too inefficient to be a sole energy source. Thus, in aerobic organisms, there is a critical size, above which it becomes essential to utilize a system for bulk transport of an O_2-containing medium (Newton, 1928). By using internal convection to improve the rate at which O_2 can reach deep tissues, it allows organisms to continue to increase in size well beyond the limits defined by simple diffusion. What is currently debated however, is where precisely this size limit exists for small but complex organisms.

1.3 The Circulatory System

Vertebrates utilize a circulatory system to achieve internal convection and thus overcome the constraints of diffusion limiting the supply of O_2 to tissues. The circulatory system is composed of five main components; the first being the heart which acts as the pump that moves the fluid (blood) around the body. The second component is the blood itself, which acts as the medium to be pumped. The third component is the arterial system that acts as the piping network

moving the blood away from the heart and towards the surrounding tissues. The fourth component is the capillary system which is composed of small thin-walled vessels that facilitate exchange between the blood and the surrounding tissues. The capillary network also acts as the connecting link between the arterial and the fifth component, the venous system, which returns blood to the heart. Together, these components form a closed loop to move the O_2 containing medium (blood) around the body and improve the rate of O_2 distribution throughout the organism.

The efficiency of this system usually is further complemented by the means of an O_2-carrying pigment which in vertebrates, is hemoglobin. Hemoglobin raises the O_2 carrying capacity of the blood thus increasing the total amount of O_2 moved per given volume (Larimer, 1959). This equates to a higher efficiency as less fluid is required to be moved via convection to move the same amount of O_2 to the internal tissues (Holeton, 1970). An improved ability to deliver O_2 is one of the major ways that the circulatory system helps maximize the range of survivable external environmental conditions for an organism. It also has secondary benefits as a transportation system that aids in communication between tissues. Thus, the circulatory system conveys signals throughout the body to optimize function relative to the external environmental conditions. The circulatory system achieves these roles by functioning in gas transport, pH regulation, ionic balance, and metabolite and hormone transport.

1.4 O_2 in the Aquatic Environment

Aquatic organisms may encounter environmental conditions of low O_2 (hypoxia) or even absence of O_2 (anoxia) either temporally or spatially. Because warm water has a lower O_2 carrying capacity than cold water (a result of the inverse relationship between O_2 solubility and temperature), the warming water bodies associated with climate change further increases the occurrence of hypoxic conditions (Conley et al., 2011; Diaz & Breitburg, 2009; Matear & Hirst, 2003; Naqvi et al., 2000). With O_2 being an indispensable commodity for aerobic respiration in most large vertebrates (Jonz & Nurse, 2006), the ability to sense O_2 availability is a highly beneficial asset. It allows organisms to respond to decreasing environmental O_2 and mount an adaptive response to either improve O_2 extraction efficiency or move to an area of higher O_2 content (Perry & Gilmour, 2010; Perry & Tzaneva, 2016).

Zebrafish (*Danio rerio*) are a tropical freshwater teleost species native to the southeastern Himalayan region (Engeszer et al., 2007). They typically inhabit slow moving water beds such as ditches and rice fields. Both of these environments are prone to prolonged bouts of hypoxia due to high environmental temperatures and stagnation of the waterways (Engeszer et al., 2007). This demanding natural environment make zebrafish an interesting model organism to study the limits of O_2 transport and sensing capabilities in teleost fish. Zebrafish larvae (typically less than 4 days post fertilisation; dpf) are also small (~4.5 mm x 0.5 mm) but develop a high level of complexity without large increases in size. This makes them an excellent model for examining the threshold where size becomes limiting for O_2 uptake without the need for internal convection. Zebrafish have the additional benefits of being amenable to a high diversity of genetic tools, ease of raising and breeding in captivity, and translucent larvae, which further facilitate their use as a model to study these questions.

Zebrafish sense environmental O_2 by using chemosensory cells called neuroepithelial cells (NECs) (Jonz & Nurse, 2003). Activation of NECs by aquatic hypoxia initiates a cascade of cardiorespiratory responses aimed at ameliorating the disruptive effects of hypoxia on metabolism (Perry et al., 2009). Although NECs can trigger the hypoxia response, the full signaling pathway is not yet well understood. It is known that these cells contain the neurotransmitter serotonin (5-HT) that is thought to be released upon stimulus induced membrane depolarization and which may interact with proximal nerve terminals (Coccimiglio & Jonz, 2012; Jonz et al., 2015). The efferent pathway that yields the hypoxia response, however, is still not well explained.

The NECs themselves are innervated and appear on zebrafish gill arches as early as 3 dpf and on the gill filaments by 5 dpf (Coccimiglio & Jonz, 2012; Jonz & Nurse, 2005). Prior to their appearance on the gill, NECs are found on the skin as early as 24 hours post fertilisation (hpf) and are capable of inducing a hypoxia response by 48 hpf (Coccimiglio & Jonz, 2012). The cutaneous NECs that develop during the first 24 hours increase in numbers until peaking around 3 dpf under normal conditions. At this point, there is a transition period where the cutaneous NEC population begins to decline gradually while a NEC population on the gill arch starts to develop and increase in size (Coccimiglio & Jonz, 2012; Jonz & Nurse, 2005). The progressive loss of the cutaneous population after the early larval stages coupled with its early development suggest that the ability to sense environmental O_2 is of similar importance in larval fish as it is in adults.

Although the developmental timeframe for NEC expression is documented, the mechanisms underlying the spatial shift from skin to gill are not well understood. It was shown

that hypoxia prolongs the existence of the cutaneous NEC population. Normally the cutaneous NECs demonstrate a decrease in mitotic cells which is accompanied by a corresponding decline in population beyond 3 dpf. Hypoxic exposure during development however increases the number of mitotic cutaneous NECs resulting in increased NEC proliferation and a larger overall cutaneous NEC population (Coccimiglio & Jonz, 2012; Dean et al., 2017). NEC development likely depends on various transcription factors however to date these factors have yet to be identified. It is possible that internal convection may play some role in the transport of these transcription factors and through this role, internal convection may impact both NEC development and spatial orientation. If loss of internal convection impedes transport of key transcription factors for NEC development there could potentially be a reduction or loss of the hypoxia response.

In larval zebrafish, the heart is fully formed and begin beating as early as 24 hpf, before the fish are motile or exhibit a touch reflex (Kimmel et al., 1995). Blood vessels start to form as early as 19 hpf including main blood vessels such as the common cardinal vein, the cardinal artery, as well as some axial and trunk vasculature (Westerfield et al., 2015). The rapidity with which the circulatory system develops suggests that it may be of similar importance in larval zebrafish. On the other hand, it is well established that during early development, larval zebrafish depend primarily upon their body skin as the principle site for O_2 uptake (Rombough, 2002). This situation contrasts markedly with the adult fish which utilize the gills as the primary site for O_2 uptake. Thus, while adult zebrafish must rely on internal convection (blood flow) to deliver O_2 from the gill to the periphery, a similar requirement for internal convection may not

exist in the larvae because the entire body surface area is capable of extracting O_2 and thus delivery distances may be short enough for diffusion, alone.

1.5 Carrier Pigment Ablation Studies

In zebrafish larvae raised in either 2% carbon monoxide (CO) or the hemolytic agent phenylhydrazine, O_2 consumption proceeds at normal rates from 36 hpf – 11 dpf (Jacob et al., 2002; Pelster & Burggren, 1996). Both of these treatments prevent haemoglobin from participating in blood O_2 transport owing either to red blood cell destruction (phenylhydrazine) or functional elimination of haemoglobin by preventing O_2 binding (CO). These treatments vastly reduce the O_2 transportation abilities of the circulatory system as O_2 physically dissolved in plasma accounts for less than 5% of the total O_2 carried within whole blood (Larimer, 1959; Pitman, 2011). Pelster and Burggren (1996) used these techniques to demonstrate that there was no variance in heart rate, swim bladder fill rate or net O_2 consumption in comparison to control larvae from 36 – 96 hpf. Similarly, Jacob et al. (2002) found that larvae raised in either 2% CO or phenylhydrazine demonstrated no significant change in cardiac rate, output or whole body lactate levels until 11 dpf.

At these young larval stages, the value of an O_2 carrying pigment is questionable during normoxia or even mild to moderate hypoxia. Similar to Pelster and Burggren (1996), Rombough and Drader (2009) further reinforced this notion by observing that there was no impact on resting O_2 consumption or critical PO_2 (the PO_2 where an organism can no longer maintain O_2 uptake independent of environmental O_2) associated with functional Hb ablation in larval zebrafish from 5 – 42 dpf. There was however a significant decrease in performance during

severe hypoxia. Rombough and Drader (2009) found that the residual O_2 leftover when the larvae could no longer extract further O_2 and thus succumbed to the hypoxia, was significantly lower in larvae with functional hemoglobin. This finding suggests that there may be a role for hemoglobin under hypoxic conditions somewhere below the critical PO_2 of the organism. The value of this benefit however compared to the cost of producing and maintaining hemoglobin during early life remains questionable.

It is important to emphasise that the studies incorporating functional ablation of hemoglobin, while demonstrating convincingly that normal rates of metabolism in developing zebrafish could be sustained by O_2 physically dissolved in the plasma, they provided no data on whether or not internal convection was required.

1.6 Antisense Morpholino Techniques

This study relies largely upon the use of antisense morpholino knockdown techniques to achieve functional phenotypes that lack internal convection. Translation blocking morpholino knockdowns use a morpholine ring sequence that is antisense to the target mRNA. The morpholino oligonucleotide sequence binds to the mRNA of interest which inhibits translation of the mRNA into the active protein and promotes degradation of the mRNA (Eisen & Smith, 2008). The cellular impermeant oligonucleotide morpholino solutions are injected into fertilised embryos during the 1-cell stage and thus spread throughout all the tissues of the organism as cells divide. The morpholinos are extremely resistant to degradation which typically allows a single injection at the 1-cell stage to inhibit mRNA translation over a 4-day period.

Two knockdown strategies were used in this study; the first approach used a translational blocking morpholino designed to target the thin filament contractile protein cardiac troponin (TNNT2, accession # NM_152893) gene in zebrafish (Sehnert et al. (2002) expressed in heart muscle sarcomeres. Mutations in the TNNT2 gene have been linked to hypertrophic cardiomyopathy, the leading cause of sudden death in young athletes (Maron et al., 1996), and dilated cardiomyopathy (Thierfeider et al., 1994) a leading cause of heart failure. Sehnert et al. (2002) demonstrated that the absence of cardiac troponin in zebrafish resulted in the destabilization and degradation of all the connective filament proteins forming the cardiac sarcomere. This degradation resulted in a non-beating heart defined as a 'silent heart' (*sih*) mutation. These TNNT2 mutants, despite the absence of a functional heart, were able to survive for 7 dpf. The findings of Sehnert et al. (2002), and (Habeck et al., 2002), coupled with the earlier hemoglobin ablation studies, have further fuelled speculation about the necessity of circulation during early embryonic/larval development in zebrafish. The second morpholino knockdown targeted the protein vascular endothelial growth factor (VEGF; accession # NP_571483) which is critically involved in angiogenesis, the formation of blood vessels. This translation blocking morpholino was originally adapted for use in zebrafish by Habeck et al. (2002) from a translational blocking morpholino knockdown VEGF-A, originally designed for mice (Driver et al., 1999). In their study, larval zebrafish at 2 dpf exhibited major blood vessel deficiencies including absence of axial and intersegmental vasculature, with no, or greatly reduced, numbers of circulating blood cells depending on the dose of morpholino used.

1.7 Hypotheses

The importance of O_2 is paramount in vertebrates to supply their energetic demands through aerobic mitochondrial respiration. Although O_2 transfer across respiratory structures (lungs, gills and skin) is achieved ultimately by passive diffusion of O_2, most multicellular organisms cannot survive on passive diffusion alone, but require internal fluid convection to i) rapidly remove O_2 from the site of transfer and thus sustain diffusion gradients near their exchange surface and ii) deliver O_2 to sites far removed from the specialised respiratory surfaces. Aquatic organisms in particular, are challenged due to the lower O_2 carrying capacity, permeability and diffusion rates in water when compared to air. The size limitation for simple diffusive gas transfer (no internal convection) is explained through the relative surface- to-volume argument (see above) where internal volume rapidly outpaces external volume at a rate of 3:2 as size increases. The size however, where simple diffusion becomes limiting for a small but complex organism, is not known. In larval zebrafish, a decrease in O_2 carrying capacity through loss of haemoglobin only affects extreme hypoxia performance and has no effect on resting O_2 consumption. These findings suggest that ultimately a carrying pigment may not be required at such small sizes, however it begs the question about convection itself.

This leads to the first hypothesis that **larval zebrafish require internal convection for maintenance of resting aerobic metabolic rate**. It is predicted that loss of internal convection will decrease resting O_2 uptake and carbon dioxide excretion rates.

Knowing that the presence of haemoglobin benefits $\dot{M}O_2$ during hypoxia when the critical PO_2 is passed, one can logically predict that loss of internal convection would further

impact hypoxia performance in larval zebrafish. The effect of this loss may even continue to impact performance beyond extreme hypoxia to more moderate hypoxia. This leads me to question the impact of internal convection on the hypoxic response in larval zebrafish.

This idea is explored in the second hypothesis that **loss of internal convection will reduce acute hypoxia performance under moderate hypoxia conditions**. It is predicted that due to transport impediment of the transcription factors critical for NEC development there will be a blunted hypoxia response and decreased NEC density.

CHAPTER 2

Internal convection and resting gas transfer in larval zebrafish

(*Danio rerio*)

2.1 INTRODUCTION

Oxygen (O_2) is a critical component for life and ensuring a sufficient supply of O_2 to metabolising tissues is paramount. O_2 transfer is diffusive in nature, its net direction and rate of movement are dictated by partial pressure gradients. Thus, O_2 will naturally flow from the external environment towards its site of consumption, the mitochondria, resulting in steadily decreasing levels of O_2 as it travels away from its site of entry, typically a specialised respiratory structure optimised for gas transfer. Consequently, aerobic metabolic rates ultimately are limited by the ability of an organism to supply O_2 to its tissues and to remove the gaseous end-product of aerobic respiration, CO_2. Similar to O_2, the transfer of CO_2 also is diffusive in nature, however, CO_2 has a capacitance in water that is roughly 30 times greater than O_2 (Boutilier et al., 1984) owing to its hydration to bicarbonate (HCO_3^-), which is the major component of total CO_2 in water. The lower capacitance of O_2 in water reflects the fact that it is carried solely as physically dissolved (gaseous) O_2. A consequence of the higher capacitance of CO_2 in water is that for equivalent partial pressure gradients, the rate of CO_2 diffusion will exceed that of O_2 diffusion.

In small organisms, a high surface-to-volume ratio allows passive diffusion, alone, to supply sufficient O_2 to the depths of an organism. As animals increase in size however, surface-to-volume ratios decrease and their increasing structural complexity is accompanied by the formation of additional barriers that are less permeable to O_2. Effectively, simple diffusive O_2 transfer in larger organisms is constrained by two factors. First, the principal driving force for diffusion, partial pressure gradients, normally maintained in small organisms by diffusive uptake of O_2 into nearby metabolising cells, are difficult to sustain because the sites of cellular

metabolism may be far removed from sites of O_2 uptake. Second, regardless of partial pressure gradients, the distances required for O_2 molecules to travel from sites of uptake to regions of metabolism will quickly exceed the rate limits of diffusion, alone. For similar reasons, the reliance on simple CO_2 diffusion, alone, to meet CO_2 excretion requirements, also is constrained by increasing size.

The ability of large and complex vertebrates to achieve high rates of O_2 uptake and CO_2 excretion is assured by their use of internal convection (circulation). Internal convection allows for the rapid movement of O_2 and CO_2 within the organism at much greater rates than would be allowed by simple diffusion, alone while concurrently sustaining diffusion gradients by dissipating O_2 and CO_2 molecules that otherwise would accumulate at sites of entry and formation, respectively.

Historically, it has been suggested that in larval fish, body diameters under 1 mm are sufficiently small to rely solely upon passive diffusion (Burggren & Pinder, 1991). Larval zebrafish (*Danio rerio*) at 4 days post fertilization (dpf) are relatively small, being 3-4 mm long and about 0.5 mm in diameter. These dimensions theoretically place them within a zone to be entirely reliant upon simple diffusion for gas transfer and transport. In larval fish it is also generally assumed that the primary site of gas transfer is the skin (Burggren & Pinder, 1991; Wells & Pinder, 1996) and larval zebrafish are no exception to this rule (Rombough, 2002).

Hemoglobin (Hb) ablation studies performed on larval zebrafish by Pelster and Burggren (1996) and Jacob et al. (2002) revealed that Hb is not required for resting O_2 uptake in larval zebrafish from 36 hours post fertilisation (hpf) until 11 dpf. It is important however, to

distinguish between the presence of an O_2 carrying pigment such as Hb, which can obviously enhance internal O_2 transport, and circulation, itself. Although respiratory pigments are of critical importance in raising the O_2-carrying capacity of the blood and thus permitting high metabolic rates, the absence of circulation, even in the presence of respiratory pigments may impede diffusive gas transfer in zebrafish larvae owing to the dissipation of partial pressure gradients. Furthermore, the lack of convection may impede the internal transport of respiratory gases. Therefore, the results of the previous Hb ablation experiments, while demonstrating that larval zebrafish do not require carrier pigments for O_2 uptake at rest under normoxic conditions, did not provide any data on the necessity of internal convection, *per se*. Consequently, there is a critical gap in our understanding of the respiratory physiology of larval zebrafish despite its emerging role as a model organism to study the ontogeny of cardiovascular biology in vertebrates (Bakkers, 2011; Nguyen et al., 2008). Specifically, nothing is known concerning the importance of internal convection of blood in allowing normal rates of O_2 uptake and CO_2 excretion. With this background, the goal of the current study was to test the hypothesis that internal convection is required for maintenance of resting aerobic metabolic rates in larval zebrafish. To test this hypothesis, O_2 consumption and CO_2 excretion were assessed in fish with and without functional circulatory systems.

2.2 MATERIALS AND METHODS

2.2.1 Fish Care and Breeding

Wild type zebrafish were raised in the University of Ottawa aquatic care facility. The adults were housed in 10 L acrylic tanks in closed, re-circulating flow-through aquatic housing systems (Aquatic Habitats, Apopka, FL, USA). The housing systems were supplied with aerated dechloraminated City of Ottawa tap water and maintained on a 14h:10h light:dark cycle at 28°*C* (Lawrence, 2007). For controlled breeding, two females and one male were placed into a breeding trap for 9 - 16 h where they were physically separated using a clear plastic divider. The following day within 1.5 h from the start of the light cycle, the water was changed and the divider of the trap was removed, allowing for breeding to occur. After 10 min, the embryos were collected from beneath an inner insert fitted with a perforated floor using a fine mesh strainer and placed into Petri dishes containing E3 embryo medium (4.9 mM NaCl, 0.16 mM KCl, 0.33 mM $MgSO_4$, 2.9 mM $CaCl_2$; Nusslein-Volard & Dahm, 2002). After hatching (usually around 48 h post fertilization; hpf), the larvae were raised in the dark, unfed in 60 ml Petri dishes for no longer than 144 hpf. All procedures for animal use were carried out in compliance with the University of Ottawa Animal Care and Veterinary Service (ACVS) guidelines under protocol BL-226 and in accordance with the recommendations for animal use provided by the Canadian Council for Animal Care (CCAC).

2.2.2 Morpholino Micro-Injections and Embryo Care

Functional elimination of internal convection was achieved using two different antisense morpholino oligonucleotide sequences purchased from GeneTools (Philomath, OR, USA). In one

group, embryos were injected with a morpholino oligonucleotide sequence (5'-CATGTTTGCTCTGATCTGACACGCA-3') targeting the translation start codon and flanking 5' sequence of the TNNT2 gene; these fish are hereafter referred to a TNNT2 morphants. These TNNT2 morphants are characterized by dysregulation of the cardiac thin filament proteins, cardiac sarcomere loss and a non-beating or 'silent' heart (*sih*) (Sehnert et al., 2002). In another group, embryos were injected with a morpholino oligonucleotide sequence (5'-GTATCAAATAAACAACCAAGTTCAT-3') targeting the translation start codon of the vascular endothelial growth factor (VEGF-A) gene (Nasevicius et al., 2000); these fish are hereafter referred to as VEGF morphants. These VEGF morphants are characterized by reduced and/or absent axial and intersegmental vasculature, resulting in an incomplete circulatory loop (Nasevicius et al., 2000). On each day of injections, a separate group of sham embryos was injected with a morpholino sequence (5'-CCTCTTACCTCAGTTACAATTTATA-3') targeting human beta globin (accession #AH001475 M34058 M34059), a gene not known to exist in the zebrafish genome and thus serving as a control for the effects of injection and morpholino loading. Before injection, the solutions were preheated to 65°*C* for 10 min. The working stock of the morpholinos was 2 ng nl^{-1} with 1 nl (2 ng) being injected into each embryo using an IM-300 Narishige programmable micro-injector (Narishige International USA Inc, Amityville, NY, USA) and glass pulled capillary needles which were calibrated for injection volume using a bolus injection radius and the equati*on* $V = 4/3\pi r^3$. The morpholino stock was diluted in 1x *Danio* buffer [5.0 mM Hepes (pH 7.6), 58 mM NaCl, 0.4 mM $Ca(NO_3)_2$, 0.7 mM KCl, and 0.05% phenol red]. To facilitate injections, the embryos were placed onto 2% agar moulds. All three morpholino sequences contained a 3'-flourescein tag that allowed for visual confirmation (at 24

hpf) of successful integration into the developing embryo. After injection, embryos were placed into 60 ml Petri dishes (approximately 30 embryos per dish) containing E3 medium or dechloraminated water supplemented with 0.5 mg/L of the antiseptic methylthioninium chloride (Methylene Blue) and reared at 28.5°*C* up to 6 days post fertilization (dpf). The E3 embryo medium or fresh systems water was replaced every 24 h.

2.2.3 Phenotype Confirmation

TNNT2 knockdown was verified by visualizing the larvae with a dissection microscope at 4 dpf and confirming the absence of a beating heart. VEGF-A knockdown was confirmed by visualizing fluorescently labelled microspheres in the circulatory system. A 50% solution (diluted in 1% bovine serum albumin; BSA) of 0.045 µm fluorescently tagged microspheres (Fisher Scientific, Waltham, MA, USA; prod # F8793) was injected into the heart of the 4 dpf larvae using an IM-300 Narishige programmable micro-injector (Narishige International USA Inc, Amityville, NY, USA) and glass pulled capillary needles which were calibrated for volume injected using a bolus injection radius and the equation $V = 4/3\pi r^3$. After injection, the larvae were imaged under a Carl Zeiss confocal microscope (Carl Zeiss Meditec Inc, Dublin, CA, USA) to examine the distribution (or lack thereof) of fluorescence throughout the vascular system (excitation 580 nm, emission 605 nm)

2.2.4 Visualization of Red Blood Cell Movement

Larvae at 4 dpf were anesthetized using 0.3 mg ml^{-1} tricaine methanesulfonate (MS-222; Syndel Laboratories Ltd., Nanaimo B.C., Canada) solution, and visualized using a Nikon SMZ 1500 microscope (Nikon Instruments, Melville, NY, U.S.A.) with a digital video camera running

OpenEye software (OpenEye Scientific, Santa Fe, NM, USA) on a personal computer. Videos were taken of the blood flow in the head, heart/yolk, and trunk regions.

2.2.5 Developmental Matching

Individual larvae at 4 dpf were imaged using a Nikon SMZ 1500 microscope coupled with a MTI DC 330 microscope camera (Meyer Instruments Inc., Houston, TX, U.S.A.). Nikon PowerDirector software was used to capture and record the images. The images were taken at 1x magnification and then compared to a ruler image taken at the same magnification. Image-J 1.51 open source software was used to measure the relative distances for each image. Then, using the ruler distance of 1 mm, the relative distances were converted into actual distances. The body length distances were measured from the mouth of the fish to the tip of the tail. The body width was assessed as the longest straight-line distance, measured from the ventral side of the yolk sac to the dorsal side of the larvae. The diameter of the eye was measured and, assuming that each eye is a sphere, the volume was calculated using the equation $v = 4/3\pi r^3$. Larvae also were imaged at 60 h to confirm presence of the long-pec pectoral fin stage, a common developmental marker (Kimmel et al., 1995).

To determine their wet mass, 30 larvae (4 dpf) were placed into pre-weighed micro-centrifuge tubes (1.5 ml) that were modified for weighing by cutting the bottom off and replacing it with fine silk mesh, secured in place by acrylic enamel. Each tube was centrifuged at 500 rpm for 4 intervals of 2 sec each, where the bottom of the mesh was dabbed on a ^{TM}KimWipe between each interval to wick away excess moisture. The larvae were then weighed on a Sartorius ED124s digital analytical balance (Weender Landstr. 94-108, 37075

Goettingen, Germany). To determine dry mass, 4 dpf larvae were placed into pre-weighed 1.5 ml eppendorf tube in a ratio of 60 larvae per tube; excess water was removed via micropipette. The tubes were placed in a heat block set at 65°*C* with the caps open. The block was covered with 2 sheets of paper, one horizontally and one vertically, forming a dome of paper that acted as the drying oven. The dome was then perforated with three ¼-inch holes to ensure ventilation. The larvae were left to dry for 72 h. After drying, the larvae were weighed on a MX5 Microbalance (Mettler Toledo, Columbus, USA).

2.2.6 Micro-respirometry

To measure O_2 consumption and CO_2 excretion rates, 30 larvae (4 dpf) were pooled in a glass micro-respirometry chamber (2.94 ml volume; Loligo Systems, Tjele Denmark). Each chamber was equipped with a mini-magnetic stir bar separated from the larvae by a stainless-steel mesh. The stir bar spun at 400 rpm using a mini-magnetic stir system (Loligo Systems, Tjele Denmark). Each chamber was filled with freshly aerated system water, replaced and refilled 3 times to ensure complete homogeneity of gases throughout the mini-respirometry chamber. The entire system was submerged in a water bath, which was maintained at 28.5°*C*. Uniform temperatures within the bath were assured by using a small aquarium pump to circulate and mix the water. Water PO_2 was monitored using fibre-optic O_2 electrodes (FOXY AL-300; Ocean Optics, Dunedin, FL, U.S.A.) and a laptop PC running the corresponding Ocean Optics Software. The electrodes were calibrated before each experimental trial using a zero-solution containing 20 g l^{-1} of anhydrous sodium sulphite and freshly aerated water (153 Torr). Prior to beginning continuous real-time measurements of water PO_2, samples (3 X 50 µl) were withdrawn from the respirometry chamber using gas-tight Hamilton syringes. These 3 samples

were used to measure the average initial total CO_2 content of the water, using a custom built total CO_2 analyser with the capacity to detect 6.8 μmol L^{-1} (0.3 ppm) CO_2 content. The design of the total CO_2 analyzer was based upon Cameron Instruments Capni-Con total CO_2 analyser (Cameron Instruments Inc., Guelph, ON, Canada); The instrument was designed and built by the electronics shop of the Faculty of Science at the University of Ottawa. After withdrawing water samples in triplicate, a fiber-optic O_2 probe was inserted into the chamber which was topped up with freshly-aerated water, and sealed. Once the probe was inserted and the readings had stabilized (normally within 2 min), PO_2 was recorded continuously for 30 min. After 30 min, additional water samples (3 X 50 μl) were removed from the chamber and analysed as above to yield final total CO_2 levels. O_2 consumption ($\dot{M}O_2$) was calculated as the average rate of PO_2 change in the chamber (2ml vol.) over time. The average slope during the 30 min experiment was taken and subsequently converted to μmol of O_2 using the conversion factor of 1.5906 μmol O_2 torr L^{-1}. CO_2 excretion ($\dot{M}CO_2$) was calculated as the net change in total CO_2 levels between the initial and the final water samples. A respirometry exchange ratio (RER) was calculated using the formula RER = $\dot{M}CO_2/\dot{M}O_2$.

In a separate series of experiments designed to assess the possible contribution of reduced activity in the morphants to decreasing rates of gas transfer, all larvae were immobilized in an aerated MS-222 solution (0.06 mg ml^{-1}) for 5 min prior to starting respirometry. In these experiments, water in the respirometer also contained 0.06 mg ml^{-1} MS-222 adjusted (using HCl and KOH) to pH 7.4. The experimental procedures were otherwise unmodified.

2.2.7 Scanning Micro Optrode Technique (SMOT) and Regional O_2 Fluxes

Individual larvae were placed in a solution of 0.3 mg ml^{-1} MS-222 for 10 min and then transferred to the measurement dish (also filled with aerated 0.3 mg ml^{-1} MS-222) with a Sylgard 184 silicon elastomer floor (Dow Corning, Midland, MI, USA). The larvae where secured to the dish by placing a thin 'seatbelt' of Sylgard across their trunk, fixing it in place with Austerlitz 0.20 mm minutiens insect pins (Entomoravia, Slakov u Brna, Czech Republic) while their head was butted up against a larger strip of Sylgard also fixed with insect pins (Fig 2.1).

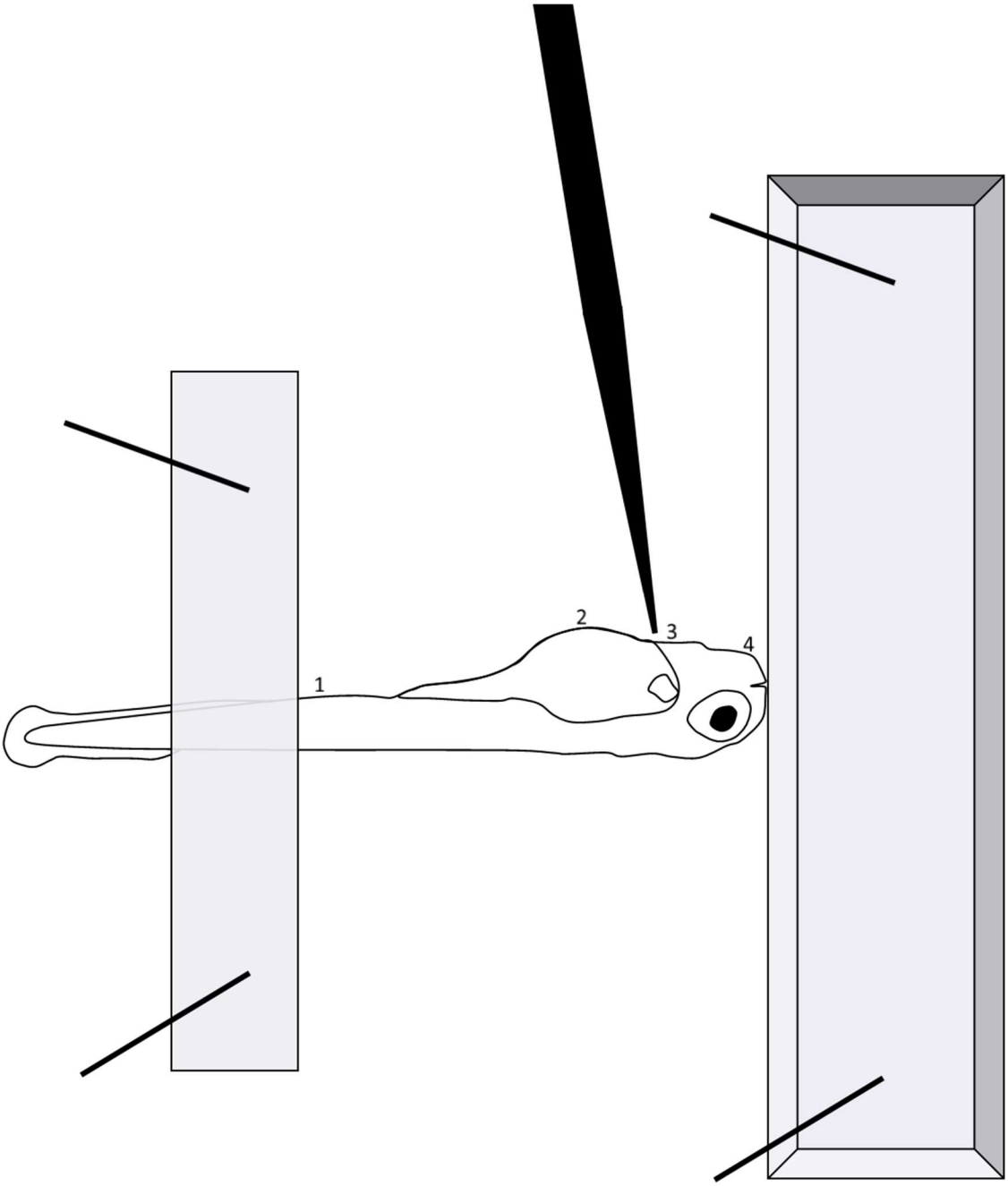

Figure 2.1 SMOT larval mounting setup and measurment locations. Fiber optrode is indicated in black, silgard blocks shown in grey and larval measurment locations numbered as follows; trunk (1), yolk sac (2), heart/gill region (3) and head region (4).

O_2 flux measurements were made using a PreSens Optrode system (PreSens Precision Sensing GmbH, Regensburg, Germany) affixed to a Nikon SMZ 1500 dissecting microscope (Nikon Instruments, Melville, NY, U.S.A.). The optrodes were prepared in house by removing the protective insulation on the cable, attaching weights to the exposed end, then heating with a handheld micro-torch to draw the fiber into a point. Tips were squared off underneath a microscope and sized at less than 50 µm in diameter using a stage micrometer. Afterward, the tips were coated with Pt(II) meso-Tetra(pentaflourophenyl)porphyrin (Pt-TFPP; Frontier Scientific, Newark, DE, USA) dissolved in chloroform and polystyrene (1 g of polystyrene in 9 g of chloroform and 25 mg Pt-TFPP). Optrode motion was controlled using a computer driven motion control unit (CMC-4; Applicable Electronics, New Haven, CT, USA) and inputs were measured using ASET-LV4 software operating on a personal computer. Measurements started at 10 µm from larval skin and proceeded to 100 µm away. Background flux measurements were taken at a distance of 3 mm away from the larvae. All measurements were repeated 5 times (technical replicates).

The SMOT technique was used to calculate O_2 flux in 4 dpf VEGF morphants and sham larvae. To do this the local PO_2 is measured at each location and then the gradient is calculated based on the delta. The delta is then corrected by subtracting the delta from the background measurement location. It is assumed that the lower PO_2 at the point nearest to the epithelium is due to the O_2 crossing the epithelium into the larvae. Using this assumption, the O_2 diffusion coefficient from Ferrell and Himmelblau (1967) and Fick's equation, O_2 flux is then calculated for the location. Four locations were selected for measurements, the head, heart/gill, yolk sac and trunk (Fig 2.1).

2.2.8 Regional O_2 Flux; Effects of Adrenaline or Heart Stoppage

Using the procedures described above, wild type (5 dpf) larvae were placed in either aerated water (control) or aerated water containing 10^{-4} M adrenaline bitartrate and 0.1 g L^{-1} ascorbic acid for 10 min. SMOT was then used to measure O_2 flux in 5 dpf larvae at 4 locations (head, heart/gill, yolk sac and trunk). Larvae were used at 5 dpf for this experiment because of their improved cardiac responsiveness to adrenergic stimulation compared to 4 dpf (Schwerte et al., 2006).

In separate experiments, a solution of MS-222 (0.6 g ml^{-1}) was added in a dropwise manner (2-3 drops every few min) until cessation of the heartbeat was achieved. The larvae were then given 5 min to adjust, followed by subsequent SMOT measurements. The media was then replaced with water lacking anaesthetic until the heart resumed beating. After 10 min, the water was replaced 3 more times and the larvae were allowed another 20 min for recovery. After the recovery, the larvae were placed in a fresh solution containing MS-222 anesthetic at the regular dose (0.3 mg ml^{-1}), given 10 min to adjust, and the SMOT measurements were repeated.

2.2.9 Statistical Analyses

All statistical analyses were performed using SigmaPlot (Version 12.2, SPSS Inc.). Data are presented as means ± 1 standard error of the mean (SEM). Results were analyzed using either t-tests, 1-way analysis of variance (ANOVA), 2-way ANOVA or 2-way repeated measures (RM) ANOVA. All ANOVAs were followed by a Holm-Sidak post-hoc test when significant differences were detected. The significant limit for all analysis was 0.05.

2.3 RESULTS

2.3.1 Developmental Matching

In comparison to the shams, the VEGF morphants were significantly shorter between 3 and 6 dpf and unlike the sham larvae, the VEGF morphants did not increase in body length over the 3-day measurement period. Consequently, the VEGF morphants at 6 dpf were shorter than the sham larvae at 3 dpf (Table 2.1). Similarly, the VEGF morphants exhibited consistently smaller eye volumes compared to the sham larvae of the same age. Moreover, the VEGF morphants demonstrated no significant increase in eye volume over time. (Table 2.1). Sham and TNNT2 morphants were compared only at 4 dpf and, similar to the VEGF morphants, the TNNT2 larvae were significantly shorter and had smaller eye volumes relative to the sham larvae of the same age (Table 2.1). Body width was assessed only at 4 dpf; both morphants were significantly wider than their respective sham larvae (Table 2.1). Wet weights, however, did not differ between the morphants and their respective sham larvae (Table 2.1). Dry weights were also not significantly different between the sham larvae and TNNT2 morphants although the VEGF morphants were significantly heavier than the shams. There was no significant difference between the VEGF morphants and the TNNT2 morphants. Additionally, the VEGF morphants developed pectoral fins, a common developmental marker, at 60 hpf in unison with the sham larvae demonstrating matched development to 60 hpf (Fig 2.3).

2.3.2 Confirmation of Knockdown and Phenotypes

In addition to being shorter and having reduced eye volumes, all of the TNNT2 morphants and 85% of the VEGF morphants developed pericardial edema by 4 dpf (Fig 2.2). The

TNNT2 larvae failed to develop a functional heart and thus the absence of a beating heart was used to visually confirm the knockdown phenotype. The VEGF morphants were characterized by an absence of circulating blood cells, a slight reduction of overall body size and typically the exhibition of an underdeveloped heart. The VEGF morphant phenotype was confirmed using two methods; most commonly, knockdown was confirmed by the absence of blood flow which could be measured qualitatively by microscopic visualisation of red blood cells (rbcs) flowing throughout the body (refer to: https://youtu.be/mat8cfpUsZY). Knockdown also was confirmed by visualizing the vasculature using microspheres injected into the heart. The VEGF morphants demonstrated an absence of any vasculature while the sham morphants had large amounts of clearly labeled vasculature (Fig 2.4).

2.3.3 Micro-respirometry

At rest, the VEGF and TNNT2 morphants demonstrated significantly reduced rates of O_2 consumption ($\dot{M}O_2$) at 4 dpf. There was no significant difference in $\dot{M}O_2$ between the VEGF and TNNT2 morphants. Similarly, there was no significant difference in $\dot{M}O_2$ between the two sham groups (Fig 2.5A). Similar responses were observed for resting CO_2 excretion rates ($\dot{M}CO_2$); the VEGF and TNNT2 morphants displayed significantly lower $\dot{M}CO_2$ relative to shams (Fig 2.5B). As for the $\dot{M}CO_2$ data, there was no significant difference between the two morphant groups or two sham groups, respectively (Fig 2.5B). Finally, there was no significant difference among the respiratory exchange ratios (RER) for any of the four groups (Fig 2.5C).

Because it was possible that the decreased rates of $\dot{M}O_2$ and $\dot{M}CO_2$ in the morphants might have been associated with reduced levels of activity in these fish, a separate series of

respirometry experiments was performed on inactive (non-motile) fish. However, despite total inactivity associated with light anaesthesia, the VEGF morphants continued to demonstrate decreased $\dot{M}O_2$ and $\dot{M}CO_2$ compared to the sham larvae (Fig 2.6).

2.3.5 Regional Oxygen Fluxes

Using SMOT to measure regional O_2 fluxes (JO_2), the VEGF morphants at 4 dpf demonstrated significantly lower JO_2 compared to the sham larvae at all four locations examined (Fig 2.7). Spatial differences in JO_2 trends were similar in all fish examined, with JO_2 being highest in the heart/gill region followed by the yolk and head regions and lowest at the trunk (Fig 2.7).

Exposure of larvae at 5 dpf to 10^{-4} M adrenaline caused a significant increase in heart rate of approximately 40 beats min^{-1} when compared to their resting baseline values (Table 2.2). However, the cardio-acceleration associated with adrenaline treatment did not affect JO_2 at any of the four locations examined (Fig 2.8).

Stoppage of the heart in sham larvae was accompanied by a significant reduction in JO_2 at the head, heart/gill and yolk regions compared to either the initial JO_2 or the JO_2 after the heart had been restarted (post-recovery). There was however, no significant decrease in JO_2 at the trunk region. There was no significant difference between the initial resting JO_2 values and the post-recovery JO_2 values at any of the 4 locations (Fig 2.9 A). In contrast, cardiac arrest in the VEGF morphants was without effect on JO_2 at any of the four measurement locations. (Fig 2.9 B).

2.4 FIGURES AND TABLES

Table 2.1 Body lengths, eye volumes, and wet and dry weight data for morphants and sham larvae between 3 and 6 days post-fertilisation (dpf). Values are shown as mean ± 1 SEM. [A] Indicates a significant difference relative to the same larval type one day earlier, while * indicates a significant difference between the morphant and the corresponding sham larvae of the same age. For body lengths and eye volume N = 15 - 20; for wet weights N = 6 – 12 and dry weights N = 6 - 7. VEGF shams and VEGF morphant body lengths and eye volumes were analyzed using a 2-way ANOVA; $P < 0.05$. All other comparisons were analyzed using either a Student's t-test (parametric data) or a Mann-Whitney rank sum test (non-parametric data).

Measurement	Larval Type	Larval Age (dpf)							
		3	P-value	**4**	P-value	**5**	P-value	**6**	P-value
Body length	VEGF sham	3.2 ± 0.1	-	3.6 ± 0.1[a]	0.023	3.9 ± 0.1[a]	0.034	4.0 ± 0.1	-
(mm)	VEGF	2.7 ± 0.1*	<0.001	2.8 ± 0.1*	<0.001	2.8 ± 0.1*	<0.001	2.9 ± 0.1*	<0.001
	TNNT2 sham	-	-	4.1 ± 0.1	-	-	-	-	-
	TNNT2	-	-	3.1 ± 0.1*	<0.001	-	-	-	-
Eye volume	VEGF sham	9.9 ± 1.1	-	15.0 ± 1.1[A]	0.01	17.0 ± 1.1	-	16.0 ± 1.1	-
(mm^3)	VEGF	4.0 ± 1.3*	<0.001	5.3 ± 1.2*	<0.001	3.4 ± 1.2*	<0.001	4.7 ± 1.2*	<0.001
	TNNT2 sham	-	-	19.0 ± 1.9	-	-	-	-	-
	TNNT2	-	-	3.8 ± 0.4*	<0.001	-	-	-	-
Body width	VEGF sham	-	-	0.51 ± 0.02	-	-	-	-	-
(mm)	VEGF	-	-	0.73 ± 0.03*	<0.001	-	-	-	-
	TNNT2 sham	-	-	0.55 ± 0.02	-	-	-	-	-
	TNNT2	-	-	0.73 ± 0.04*	<0.001	-	-	-	-
Wet larval mass	VEGF sham	-	-	0.36 ± 0.01	-	-	-	-	-
(mg)	VEGF	-	-	0.37 ± 0.02	-	-	-	-	-
	TNNT2 Sham	-	-	0.27 ± 0.04	-	-	-	-	-
	TNNT2	-	-	0.28 ± 0.05	-	-	-	-	-
Dry larval mass	Sham	-	-	57 ± 7	-	-	-	-	-
(µg)	VEGF	-	-	76 ± 1*	0.018	-	-	-	-
	TNNT2	-	-	72 ± 8	-	-	-	-	-

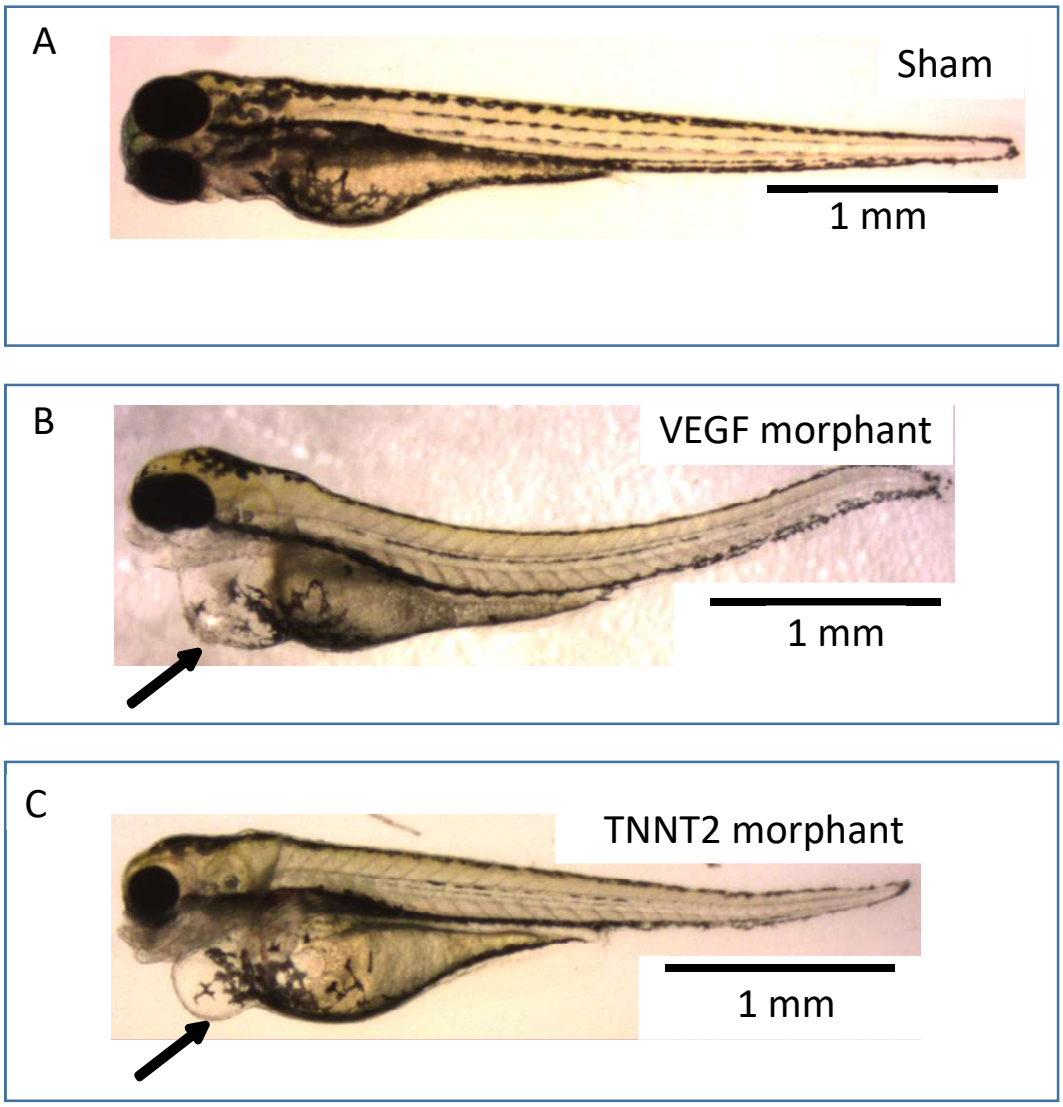

Figure 2.2 Representative microscopy images of A) sham, B) VEGF morphant and C) TNNT2 morphant zebrafish larvae at 4 days post fertilization (dpf). The black arrows indicate pericardial edema; scale bars represent 1 mm.

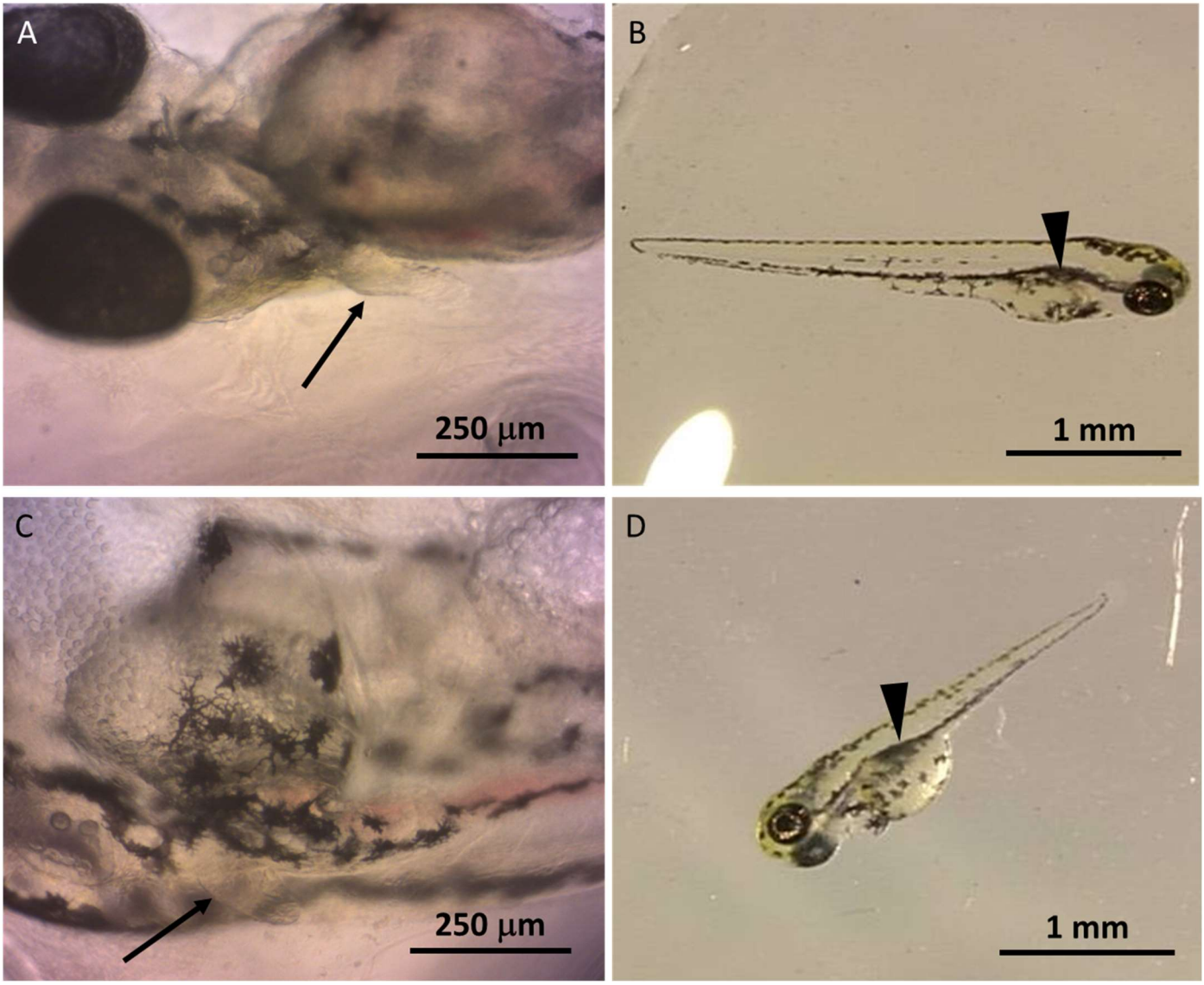

Figure 2.3. Representative microscopy images of sham (A,B) and VEGF morphant (C, D) larvae at 60 hours post fertilization (hpf) (A,C) and 72 hpf (B,D). Arrows indicate pectoral fins and arrow heads indicate melanin accumulation overlying the swim bladder rudiment.

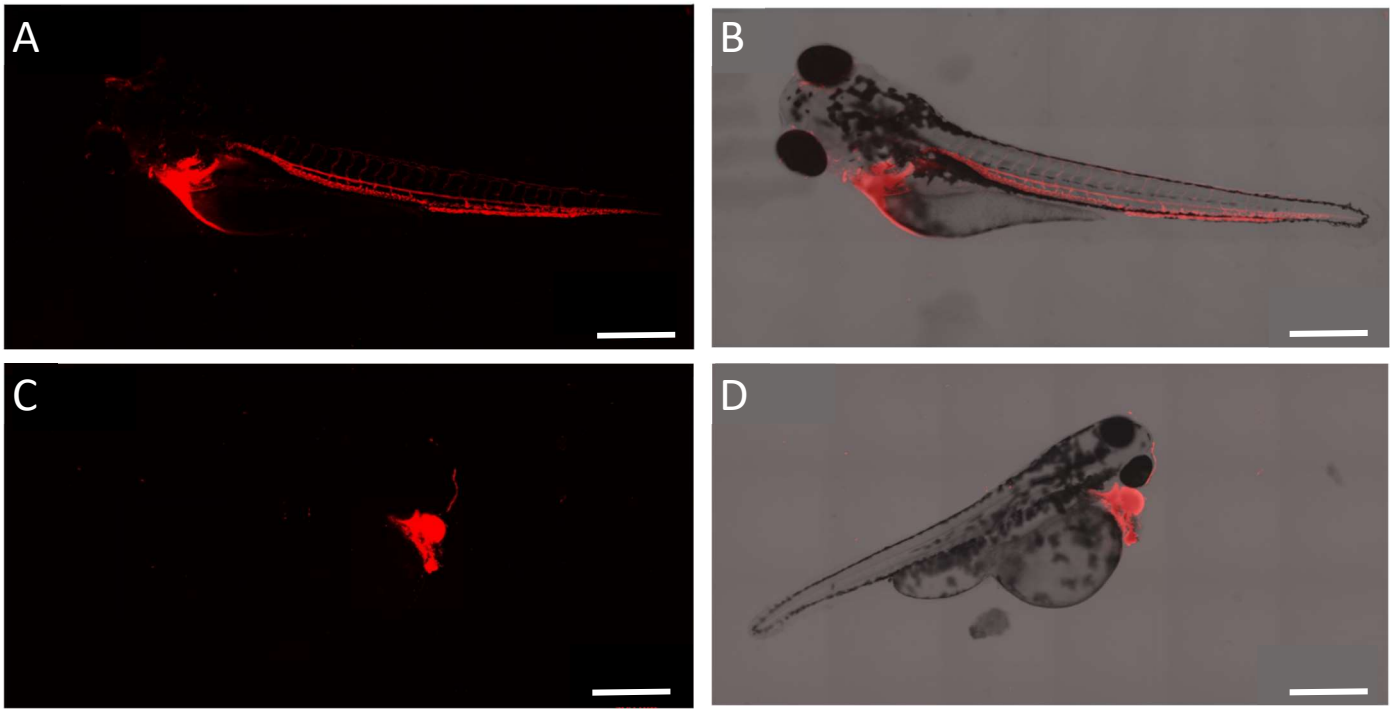

Figure 2.4 Whole body microscopic images of 4 dpf sham larvae (A, B) and VEGF morphants (C, D) injected with fluorescently tagged microspheres. Panels A and C depict fluorescence images while panels B and D depict a fluorescence and transmitted light overlay. Scale bars represent 500 µm.

Figure 2.5 Oxygen consumption rates ($\dot{M}O_2$) (A), carbon dioxide excretion rates ($\dot{M}CO_2$) (B), and the respiratory exchange ratio (RER; $\dot{M}O_2/\dot{M}CO_2$) (C) for VEGF and TNNT2 morphant larvae (4 days post fertilization) and their respective sham larvae at 28.5 *°C*. Values are shown as mean ± SEM. Letters indicate a significant difference between groups using a 1-way ANOVA.; $P<0.05$. N = 20-22. For panel A the effect of treatment was $P < 0.001$. All pairwise comparisons: sham 2 vs. TNNT2 $P < 0.001$, sham 1 vs. TNNT2 $P < 0.001$, sham 2 vs. VEGF $P < 0.001$, sham 1 vs. VEGF $P = 0.002$, VEGF vs. TNNT2 $P = 0.240$, sham 2 vs. sham 1 $P = 0.748$. For panel B the effect of treatment was $P = 0.001$. All pairwise comparisons: sham 2 vs. TNNT2 $P = 0.008$, sham 1 vs. TNNT2 $P < 0.017$, sham 2 vs. VEGF $P < 0.020$, sham 1 vs. VEGF $P = 0.034$, VEGF vs. TNNT2 $P = 0.904$, sham 2 vs. sham 1 $P = 0.816$. For panel C the effect of treatment was $P = 0.974$.

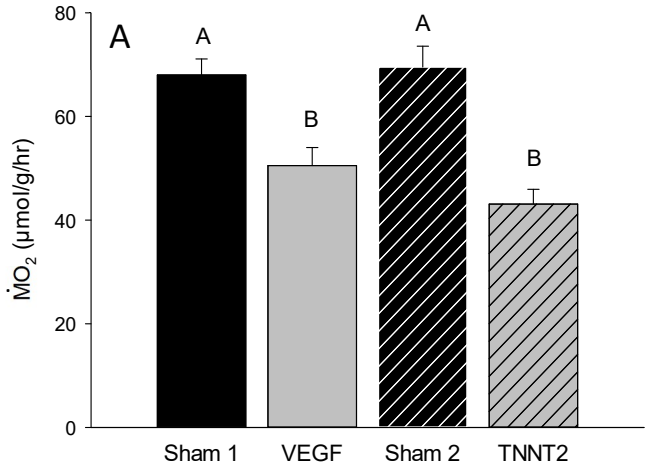
A
A
B
A
B
80
60
40
20
0
$\dot{M}O_2$ (µmol/g/hr)
Sham 1
VEGF
Sham 2
TNNT2

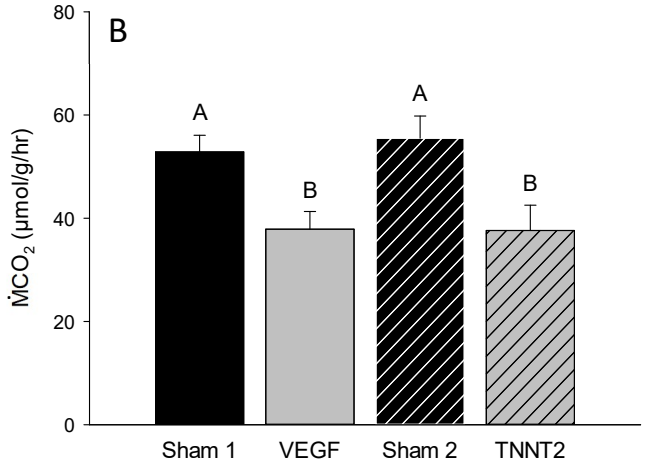
B
A
B
A
B
80
60
40
20
0
$\dot{M}CO_2$ (µmol/g/hr)
Sham 1
VEGF
Sham 2
TNNT2

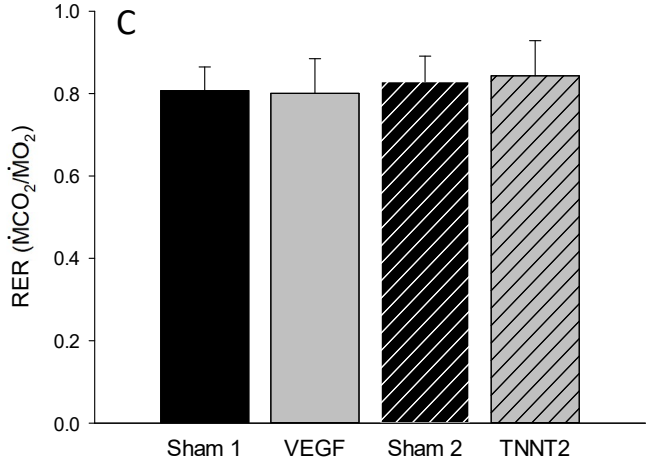
C
1.0
0.8
0.6
0.4
0.2
0.0
RER ($\dot{M}CO_2/\dot{M}O_2$)
Sham 1
VEGF
Sham 2
TNNT2

Figure 2.6 Oxygen consumption rates ($\dot{M}O_2$) (A), carbon dioxide excretion rates ($\dot{M}CO_2$) (B), and the respiratory exchange ration (RER; $\dot{M}O_2/\dot{M}CO_2$) (C) for sham and VEGF morphant larvae under light anesthetic (0.06 g L^{-1} of MS-222). Values are shown as mean ± SEM. * indicates significant differences between groups as analyzed using a Student's t-test; $P < 0.05$. N = 11. Panel A sham vs. VEGF $P = 0.030$. Panel B sham vs. VEGF $P < 0.001$. Panel C sham vs. VEGF $P = 0.984$.

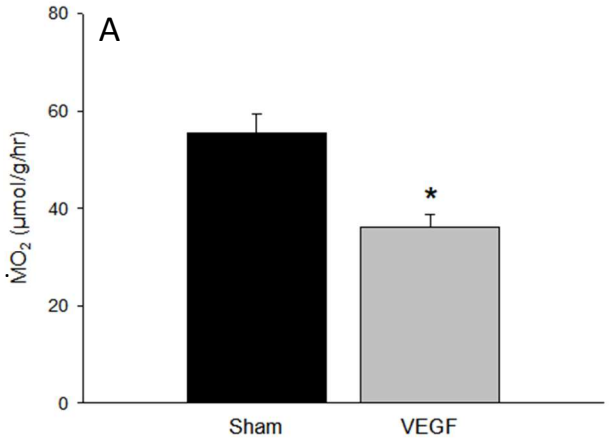
A
80
60
40
20
0
$\dot{M}O_2$ (µmol/g/hr)
*
Sham
VEGF

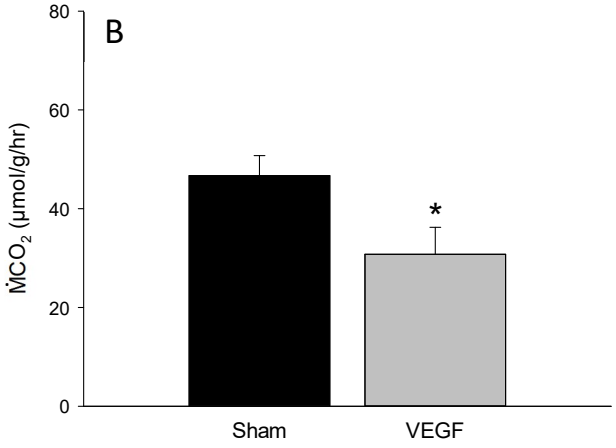
B
80
60
40
20
0
$\dot{M}CO_2$ (µmol/g/hr)
*
Sham
VEGF

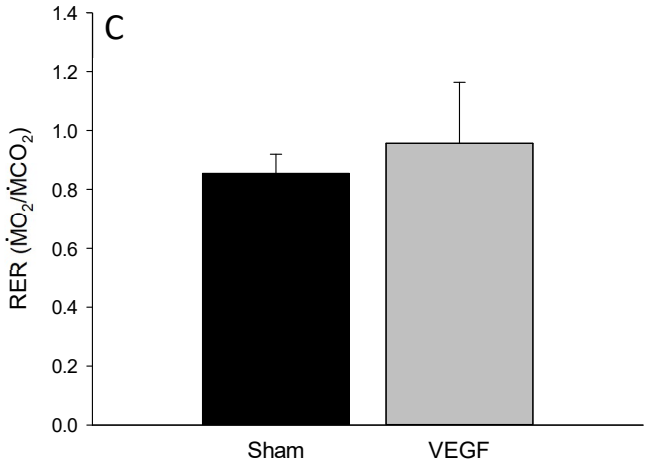
C
1.4
1.2
1.0
0.8
0.6
0.4
0.2
0.0
RER ($\dot{M}O_2/\dot{M}CO_2$)
Sham
VEGF

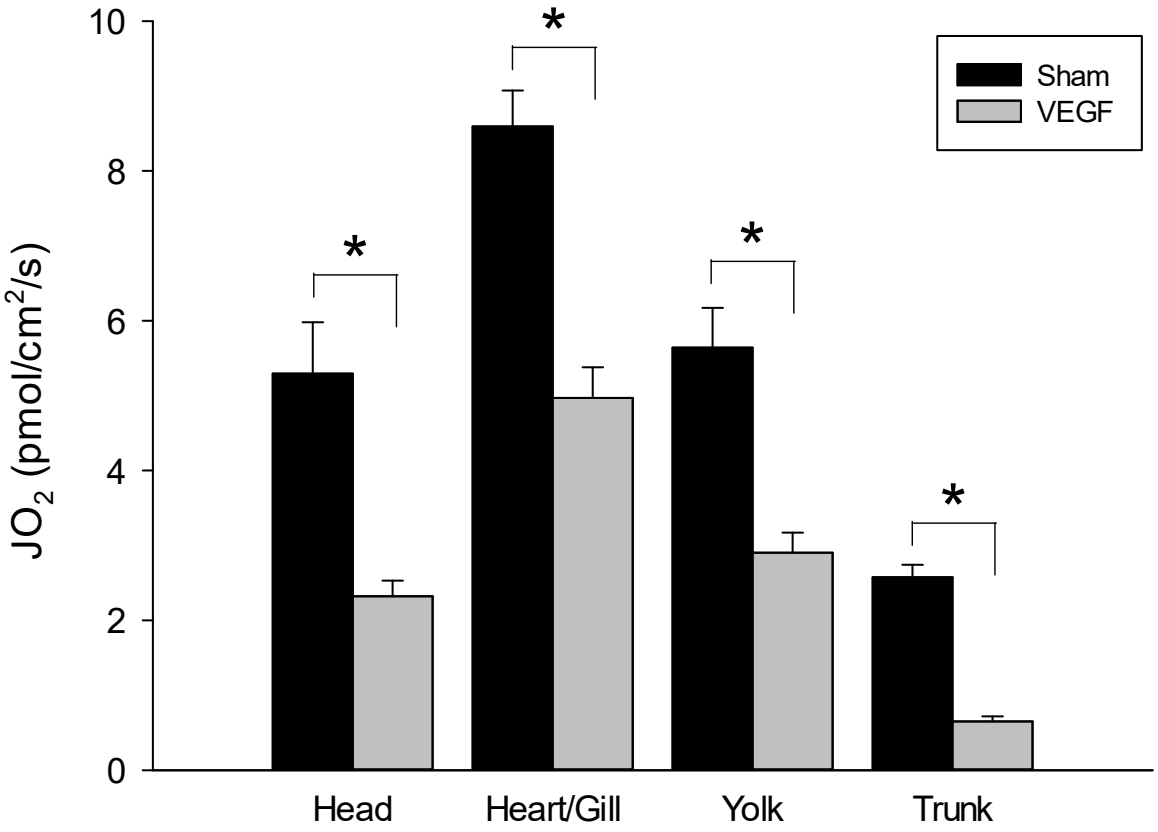

Figure 2.7 Regional oxygen flux (JO_2) for 4 dpf sham and VEGF morphant larvae. Values are shown as mean ± SEM. * indicates a significant difference between larval types at a given region as analyzed using a two-way ANOVA; $P < 0.05$. $N = 7 – 8$. Effect of larval type $P < 0.001$, effect of region $P < 0.001$, larval type x region $P < 0.001$. Comparisons within a region for sham vs VEGF: Within head region $P < 0.001$, within heart/gill region $P < 0.001$, within yolk region $P < 0.001$, within trunk region $P < 0.001$.

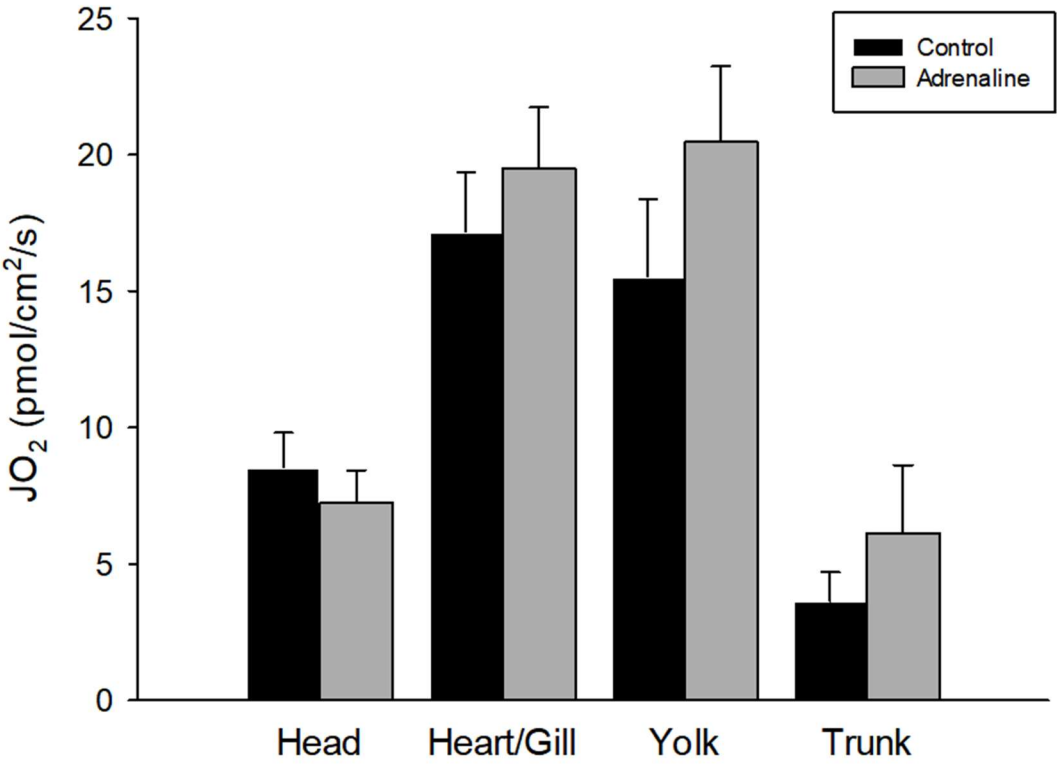

Figure 2.8 Regional oxygen flux (JO_2) for 5 dpf wild type larvae exposed to an anesthetic solution containing a control anesthetic solution without adrenaline or an anesthetic solution containing 10^{-4} M adrenaline bitartrate. Values are shown as mean ± SEM. * indicates significant differences between treatments for a given region as analyzed using a two-way ANOVA; $P < 0.05$. N = 8 - 10. Effect of adrenaline $P = 0.169$, effect of region $P < 0.001$, adrenaline x region $P = 0.560$.

Table 2.2. The effect of exposure to adrenaline (10^{-4} M adrenaline bitartrate) on heart rate (f_H) in wild type larvae at 5 days post fertilization. Values (in beats per min; BPM) are shown as mean ± SEM. * indicates significant difference between groups as analyzed using a paired Student's t-test; $P < 0.001$. N = 7.

	Pre-adrenaline	**Adrenaline**
f_H (BPM)	161 ± 12	199 ± 12*

Figure 2.9 Regional oxygen flux (JO_2) for 4 dpf sham (A) and VEGF (B) morphants with a beating heart (initial) exposed to MS-222 until the heart stopped beating (stopped) and then following a recovery phase once the heart had restarted (post-recovery). Values are shown as mean ± SEM. Different letters indicates significant differences among treatments within a given location as analyzed using a two-way RM ANOVA; $P < 0.05$. N = 5. For panel A the effect of treatment was $P = 0.003$, effect of region $P < 0.001$, treatment x region $P = 0.003$. Comparisons within a region for treatment: Within head region initial vs stopped $P < 0.001$, post-recovery vs. stopped $P < 0.001$, initial vs. post-recovery $P = 0.602$. Within heart/gill region initial vs stopped $P = 0.020$, post-recovery vs. stopped $P = 0.020$, initial vs. post-recovery $P = 0.853$. Within yolk region initial vs stopped $P < 0.001$, post-recovery vs. stopped $P < 0.001$, initial vs. post-recovery $P = 0.254$. Within trunk region initial vs stopped $P = 0.424$, post-recovery vs. stopped $P < 0.403$, initial vs. post-recovery $P = 0.853$. For Panel B the effect of treatment was $P = 0.354$, effect of region $P < 0.001$, treatment x region $P = 0.071$.

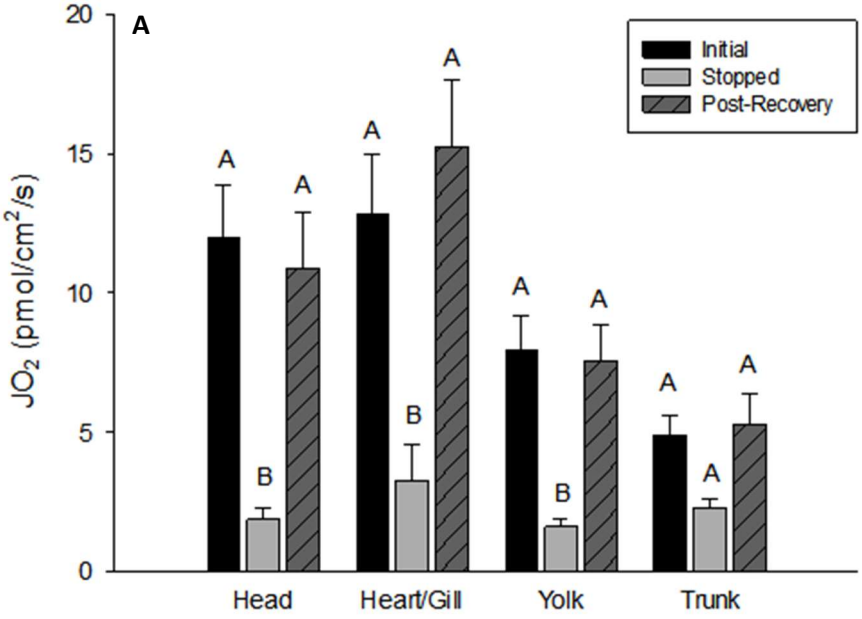
A
Initial
Stopped
Post-Recovery
JO_2 (pmol/cm^2/s)
20
15
10
5
0
A
B
A
A
B
A
A
B
A
A
A
A
Head
Heart/Gill
Yolk
Trunk

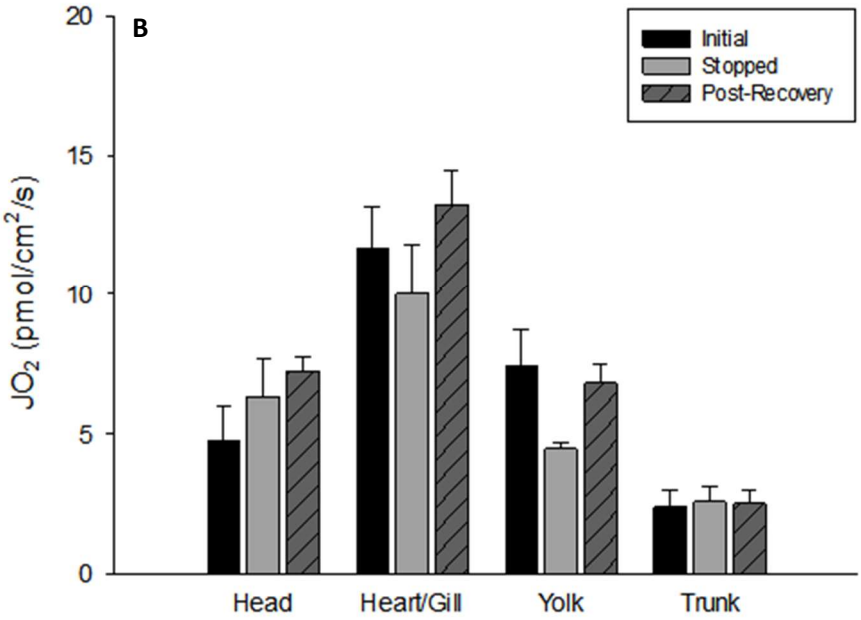
B
Initial
Stopped
Post-Recovery
JO_2 (pmol/cm^2/s)
20
15
10
5
0
Head
Heart/Gill
Yolk
Trunk

2.5 DISCUSSION

The purpose of this study was to examine the role of internal convection on respiratory gas transfer in a small but complex organism, the larval zebrafish. Based on theoretical considerations (see Dejours, 1981) and the results of previous studies (Jacob et al., 2002; Pelster & Burggren, 1996), it has largely been accepted as dogma that internal convection is unnecessary for O_2 uptake in larval zebrafish under normoxic conditions until approximately 14 dpf (Barrionuevo & Burggren, 1999; Barrionuevo et al., 2009; Jacob et al., 2002; Jonz & Nurse, 2006; Rombough & Drader, 2009). Surprisingly, however, this concept was never tested directly but rather was supported experimentally only by the results of indirect studies which assessed the physiological consequences of hemoglobin loss or its functional impairment. The results of the present study, however, provide direct evidence that internal convection is required to achieve normal rates of gas transfer in zebrafish larvae at 4 dpf and thus do not support the widely-held view that diffusion alone, is sufficient to support resting metabolic requirements in larvae.

2.5.1 Using TNNT2 or VEGF Knockdown to Prevent Internal Convection

The loss of internal convection was achieved using morpholino knockdown of two different targets; the vascular endothelial growth factor protein (VEGF) and the contractile protein cardiac troponin II (TNNT2). Both of these knockdowns achieved the same functional phenotype of eliminating internal convection, except perhaps for some mixing of the interstitial fluids that may occur with movement of the larvae. Additionally, the VEGF morphants exhibited some minor convection within the pericardium owing to the contractions of the heart. My

findings using the VEGF morphants were qualitatively similar to those reported by Nasevicius et al. (2000) but were achieved using a lower dose of morpholino (see below). Similar to the previous study, I also observed an enlarged pericardium, no circulating red blood cells (rbcs) and little or no functioning vasculature. Interestingly, despite using a lower dosage of morpholino (2 ng per embryo versus 3-18 ng per embryo), the zebrafish larvae used in the present study exhibited a greater prevalence of the 'severe phenotype' described by Nasevicius et al. (2000) characterised by the presence of heart and yolk vasculature only (or no vasculature at all) and the pumping of fluid within the pericardium. In particular, I noted a higher percentage of fish with pericardial edema when comparing similar doses of morpholino. The increased severity of the effects of VEGF knockdown observed in the current study may, in part, be associated with the greater age of the larvae examined [4 - 5 dpf in the current study compared to < 48 hpf in the study of Nasevicius et al. (2000)]. The TNNT2 morphants demonstrated similar phenotypic characteristics as described initially by Sehnert et al. (2002) consisting of a non-beating heart, loss of convection and development of pericardial edema. Similar to the previous work, the TNNT2 morphants maintained skeletal muscle as evidenced by normal hatching and motility.

Given that VEGF and TNNT2 knockdowns yielded similar effects on gas transfer, subsequent experiments were performed solely on VEGF morphants because it was felt that interpretation of the results would be more straightforward when comparing data obtained from fish with beating hearts. The VEGF morphants exhibited reduced body lengths and eye volumes, even when provided several extra days to develop; a similar effect on body length was also apparent in the original VEGF knockdown study (Nasevicius et al., 2000). The reduced

growth can be attributed to a multitude of factors, including, but not limited to, a reduced ability to transport important transcription factors and developmental hormones such as the growth hormone superfamily (growth hormone, somatolactin and prolactin), insulin like growth factor 1 (IGF1) and thyroid hormones (Liu & Chan, 2002; Moriyama et al., 2000; Zhu et al., 2007). The reduced transport abilities associated with loss of internal convection could prevent these key regulatory elements from reaching the required target tissues at the appropriate time and in the appropriate amounts. Interestingly, despite the reduced body lengths, the morphant larvae lacking circulation were equivalent (or greater) in mass to the shams owing to their increased girth (Table 2.1).

Except for the decreased eye volumes and body lengths, the VEGF morphants reached developmental milestones similarly to sham larvae. At 60 hpf pectoral fin formation was observed in shams and morphants in accordance with developmental norms (Kimmel et al., 1995) (Fig 2.3). At 72 hpf both larval types demonstrated typical melanin accumulation causing darkening over the swim bladder remnant region, increased iridophore coverage of the eye to take up more than half the eye's surface and there was apparent melanin striping of the iridophore (Kimmel et al., 1995) (Fig 2.3). Thus, based on the larval wet masses and the aforementioned developmental metrics, all fish appeared to be developmentally matched at least until 72 hpf. Although swim bladder inflation is a common marker for 4.5 dpf (Winata et al., 2009), it was not a useable marker in the current study because swim bladder inflation relies upon several convection based mechanisms and as such the swim bladder does not inflate in larvae lacking internal convection (Kuhn et al., 1963; Pelster & Scheid, 1992). Because all the major organ systems are developed by 60 hpf (Kimmel et al., 1995), and that dwarfism

aside, the VEGF morphants appear to be developmentally matched until 72hpf it is unlikely that the sham larvae and the VEGF morphants exhibited any significant differences in their expression of differentiated tissue that otherwise might have impacted metabolic rate. Thus, the metabolic needs of the tissues were presumed to be similar in shams and morphants.

Although the TNNT2 morphants were not examined directly for developmental matching, it is likely that they developed at a similar rate as the VEGF morphants given the phenotypic similarities. In light of these results and considerations, the differences observed in the aerobic metabolic rates between the morphant and sham larvae cannot be attributed simply to differences in tissue types and their subsequent impact on metabolic rate.

2.5.2 Internal Convection and Resting Gas Transfer

Although the loss of internal convection was associated with reduced resting rates of O_2 consumption and CO_2 excretion, it did not alter the respiratory exchange ratio for these two gases. Therefore, the absence of circulation appeared to affect the transfer of both gases equally and to have little, if any, effect on metabolic fuel (substrate) choice. Importantly, the magnitude of these reductions in rates of gas transfer was equivalent in both morphant phenotypes. The fact that two vastly different morpholino targets yielded such similar results strengthens the argument that the observed effects on resting gas transfer were caused by their shared functional phenotype, loss of internal convection, rather than non-specific off target effects. The current findings (at least with respect to O_2) differ markedly with the results of previous studies which reported unaltered rates of O_2 uptake in normoxic larvae lacking functional haemoglobin (Jacob et al., 2002; Pelster & Burggren, 1996). This discrepancy is hardly

surprising because there are profound differences between larvae lacking functional haemoglobin and those lacking internal convection. The predominant impact of loss of haemoglobin function is a reduction of the O_2 carrying capacity of the blood; convective fluid transport can continue to rapidly remove O_2 molecules diffusing across the skin and thus sustain PO_2 diffusion gradients while concurrently delivering O_2 to areas too distant to be effectively reached by diffusion, alone. In the strictest sense, therefore, the results of the haemoglobin ablation studies simply demonstrate that O_2 carriage in plasma is sufficient to allow normal rates of O_2 uptake in developing larvae. Therefore, the most parsimonious explanation for the differences in results obtained from the current (no convection) and previous (continuing convection) studies is that internal convection, even in larvae at 4 dpf, is required to rapidly disperse O_2 from sites of transfer and thus maximise O_2 diffusion gradients. Under normal conditions in larvae with functional haemoglobin and an intact circulation, PO_2 diffusion gradients are sustained by the combined actions of convective removal of O_2, the binding of O_2 to haemoglobin, localised O_2 consumption and diffusion of O_2.

This is the first study to assess the role of internal convection on CO_2 transfer in zebrafish larvae. In adult fish, CO_2 excretion at the gills is constrained by the need to rapidly convert plasma HCO_3^- to gaseous CO_2, a reaction which is facilitated by the presence of carbonic anhydrase (CA) in rbcs (reviewed by Gilmour and Perry, 2009). In zebrafish larvae at 4 dpf, knockdown of rbc CA caused an impairment of CO_2 excretion without affecting O_2 uptake (Gilmour et al., 2009). Thus, unlike for O_2 uptake, CO_2 excretion in zebrafish larvae appears to be reliant on the presence rbc CA produced by RBC's throughout the larvae. It is not surprising therefore, that loss of internal convection impeded CO_2 excretion in the current study because

surely normal rbc function was prevented in the absence of circulation. It is also possible that, as for O_2, the lack of internal convection leads to local accumulation of CO_2 at its production sites thereby causing PCO_2 diffusion gradients to collapse.

Although not quantified in the current study, it was apparent that the VEGF and TNNT2 morphants exhibited reduced activity compared to the sham larvae. Exercise can play a critical role in determining aerobic metabolic rate (Weibel, 1984) and differences in motility could result in differences in $\dot{M}O_2$. This idea was explored by examining the rates of O_2 uptake and CO_2 excretion in larvae under light anesthesia (to eliminate movement). The results demonstrated that the VEGF morphants continued to display decreased rates of O_2 consumption and CO_2 excretion compared to the sham larvae despite the absence of any movement in both groups (Fig 2.6). These findings support the conclusion that the reduction in resting gas transfer in the morphant larvae was caused by the loss of internal convection and was not simply a result of a lowered metabolic rate associated with decreased activity.

2.5.3 Internal Convection and Regional O_2 Transfer

No previous study has examined regional O_2 uptake in larval zebrafish nor have any examined the impact that internal convection may have on it. In this study, we utilized the scanning micro-optrode technique (SMOT) to measure the O_2 boundary layer proximal to the skin of the larval. After correction for background gradients, the PO_2 gradient in the boundary layer was used to calculate O_2 flux rates across the epithelium using Fick's equation. Using this technique, it was found that loss of internal convection caused a significant reduction in O_2 uptake at selected points along the body of zebrafish larvae.

The VEGF morphants demonstrated reduced O_2 flux rates across the epithelium at all four locations that were examined (Fig 2.7). The fact that the VEGF morphants extracted less O_2 across their skin at specific locations is consistent with their overall reduced rates of O_2 consumption. Interestingly, O_2 flux at the skin was not constant across the entire larvae as had previously been observed using a similar micro-electrode technique in trout (*Oncorhynchus mykiss*) larvae (Rombough, 1998). Indeed, in zebrafish larvae there was a notable peak in O_2 flux around the heart/gill region and a decreasing trend moving away from this point in either direction along the larvae. Loss of internal convection had no apparent impact on this trend as it was maintained in the VEGF morphants (Fig 2.7). This finding suggests that the regional flux differences observed in larval zebrafish are related to tissue demand for O_2 within the larvae and are not linked to convective differences in these regions.

When sham larvae were exposed to sufficiently high levels of MS-222 anaesthetic to acutely stop the heart, they demonstrated a reduction in boundary layer net O_2 flux at all measurement locations except the trunk. This inhibitory effect on O_2 flux could be reversed by restarting the heart by MS-222 washout (Fig 2.9A). In marked contrast, stopping the heart did not affect boundary layer net O_2 fluxes in the VEGF morphants (Fig 2.9B). These results demonstrate that the decrease in O_2 flux rate observed in the sham fish was related to the loss of internal convection; VEGF morphants were insensitive to stoppage of the heart because in the absence of pre-existing blood flow, further reductions in internal convection were not possible.

Additionally, the aerobic energetic cost of a beating heart in larval zebrafish appears to be relatively minor compared to their total aerobic energetic sum. This is supported by the lack

of any significant change in O_2 flux with a beating or non-beating heart in the VEGF morphants, in particular around the heart/gill region. This suggests that the majority of the reduced O_2 consumption observed when the heart stops is not due to the cost of the heartbeat itself, but rather the associated loss of internal convection that accompanies it.

In contrast to the pronounced effects on O_2 flux of reducing blood flow via cardiac arrest, increasing internal convection above resting had no significant impact on regional boundary layer O_2 fluxes under normoxic conditions. Thus, exposure to adrenaline did not affect boundary layer O_2 flux rates at 4 dpf (Fig 2.8) despite the significant increase in heart rate at this level of exposure (Table 2.2). These results suggest that resting rates of internal convection in larval zebrafish are either at, or above, the levels required for O_2 uptake under normoxic conditions.

2.5.4 Conclusions

Together, the results of the current study suggest that loss of internal convection causes a reduction in O_2 consumption. The most probable explanation is that loss of internal convection results in the collapse of internal PO_2 gradients and thus reduces the ability to transport O_2 from the external environment to the metabolizing tissues deep in the organism. These reduced rates of O_2 uptake and consumption could be linked to two factors. First, reduced evacuation of O_2 molecules near the epithelium likely reduces the driving gradient near the surface of the zebrafish, which effectively decreases the overall net diffusion rate. Second, because the O_2 diffusion gradient is collapsing before it reaches the center of the organism, there is less O_2 available to the tissues deep within the organism.

It is however possible that the observed reductions in O_2 consumption are related to the loss of something else, normally carried in the blood, that is critical for normal rates of O_2 consumption. One may argue that perhaps the loss of internal convection is starving the larvae for nutrients to fuel aerobic respiration. This however seems highly unlikely in light of the results from the SMOT experiments in fig 2.9 A. Given the acute loss of internal convection in the sham larvae it is unlikely that the larvae would totally exhaust all of the local nutrient stores within all of the tissues in such a short amount of time. Additionally, if nutrients were indeed limiting, one would expect to see the greatest impact of losing convection at the regions furthest from the nutrient source (the yolk sac). This trend however is not the case and there seems to be similar rates of consumption without convection regardless of proximity to the nutrient source.

The loss of internal convection reduced CO_2 excretion to an equivalent extent as O_2 uptake. However, it is unclear as to whether the decrease in CO_2 excretion was caused by a direct limitation of convection loss on cutaneous CO_2 transfer or simply an indirect and expected consequence of a decreased aerobic metabolism.

Overall, the current findings demonstrate that in a small complex organism such as the larval zebrafish, internal convection as a physical mode of O_2 transport is required to maintain resting rates of O_2 uptake and CO_2 excretion. Passive diffusion alone is insufficient to maintain internal PO_2 gradients and supply O_2 to metabolizing tissues. Ultimately, although haemoglobin may not be required under normoxic conditions, internal convection is essential to maintain resting aerobic metabolic rate in larval zebrafish.

CHAPTER 3

Internal convection and hypoxia performance in larval zebrafish

(*Danio rerio*)

3.1 INTRODUCTION

Under normoxic conditions, larval zebrafish (<14 dpf) do not require rbcs or functional haemoglobin to sustain their normal metabolic functions (Jacob et al., 2002; Pelster & Burggren, 1996). However, during acute severe hypoxia, performance indeed appears to be linked, at least in part, to the O_2 carrying capacity of the blood. This conclusion is based on the results of Rombough and Drader (2009) who observed that functional ablation of haemoglobin by carbon monoxide poisoning decreased the ability of zebrafish larvae to extract O_2 below the critical PO_2. Taken together with the results of previous studies using haemoglobin ablation techniques (Jacob et al., 2002; Pelster & Burggren, 1996), a general consensus has arisen that internal convection is not required to sustain O_2 uptake in zebrafish larvae but rather diffusion of O_2, alone, can suffice. Strictly speaking, however, the functional loss of haemoglobin serves only to reduce the O_2 carrying capacity of the blood by roughly 95%; internal convection remains intact. Indeed, the size of larval zebrafish may approach or even exceed the threshold at which simple diffusion can sustain aerobic metabolism (Dejours, 1981). This threshold however is based on extrapolation from luminous bacteria who amongst other parameters are assumed to be a perfect sphere (Newton, 1928). It has however been demonstrated that irregular geometric shapes and tissues with spatial heterogeneity significantly alter diffusion limits (Chow et al., 2001b; Grossmann, 1982). Thus, it is possible that internal convection plays an essential role in O_2 uptake in these fish by its combined effects on i) sustaining PO_2 diffusion gradients and ii) facilitating the bulk transport of O_2 to tissues otherwise unreachable by diffusion, alone. I recently provided experimental evidence supporting a significant role for internal convection in O_2 uptake in zebrafish larvae under normoxic conditions (Chapter 2).

Thus, eliminating blood flow by targeted gene knockdown of vascular endothelial growth factor (Nasevicius et al., 2000) or cardiac troponin proteins (Sehnert et al., 2002) caused significant impairment of whole body O_2 uptake and CO_2 excretion (Chapter 2). Moreover, the temporary stoppage of circulation using anaesthetic led to a reversible decrease in O_2 flux when measured in the water boundary layer adjacent to the skin; an effect which was not observed in fish already lacking a functional circulatory system (Chapter 2). The need for internal convection is expected to be even greater under conditions of hypoxia owing to a reduction in PO_2 diffusion gradients. A reduced hypoxia performance from loss of internal convection may be augmented further because of its presumed role in the development and mediation of the hypoxic cardiorespiratory responses in zebrafish larvae [(tachycardia and hyperventilation (Jacob et al., 2002; Jonz & Nurse, 2005)].

Of all the cardiorespiratory responses aimed at ameliorating the disruptive effects of hypoxia on metabolism, arguably the most important of the reflex responses is hyperventilation triggered by activation of chemosensory neuroepithelial cells (NECs) during hypoxia (Jonz et al., 2004; Jonz & Nurse, 2005; Perry et al., 2009). In adults, the increased flow of water over the gills helps to maximize the transfer of O_2 from water-to-blood in the face of declining PO_2 diffusion gradients. In larval zebrafish however, the benefit of hypoxic hyperventilation is unclear because the majority of O_2 exchange occurs over the skin, not the gills, until about 14 dpf (Rombough, 2002; Rombough & Moroz, 1997). Another predominant cardiorespiratory response during hypoxia in zebrafish larvae is an increase in heart rate (tachycardia) (Barrionuevo & Burggren, 1999; Jacob et al., 2002), which under conditions of diminishing O_2, likely increases the delivery of blood to the respiratory gas exchange surfaces while also helping

to maximise the overall water-to-blood PO_2 diffusion gradients. Although adult fish exhibit bradycardia (decreased heart rate) in response to hypoxia exposure, they typically increase stroke volume to allow an equal or greater total cardiac output despite the decreased heart rate (Randall, 1982; C. Wood & Shelton, 1980).

Thus, based on previous results (Chapter 2), it is conceivable that adjustment to blood flow may be more important than previously recognised, especially during hypoxia (Rombough & Drader, 2009). This leads to the hypothesis that ***loss of internal convection will reduce acute hypoxia performance in larval zebrafish under moderate hypoxia conditions***.

Although hypoxia responses are relatively well studied in zebrafish larvae, the efferent pathway yielding these responses is still not well understood. However, there is general agreement that the cardiorespiratory reflex responses to hypoxia are initiated by activation of the chemosensory NECs (Jonz et al., 2015; Perry & Gilmour, 2010) that ultimately promote signalling pathways involving neural and/or neurohumoral components (Coccimiglio & Jonz, 2012; Jacob et al., 2002; Jonz & Nurse, 2006). Clearly, the delivery to target tissues of any blood-borne agents involved in hypoxic signalling will be restricted in the absence of a functional circulatory system. For example, hypoxic tachycardia in larval zebrafish (at 4 dpf) presumably is mediated by the activation of cardiac β-adrenergic receptors (Schwerte et al., 2006). Given that sympathetic innervation of the heart may be absent in zebrafish larvae at 4 dpf (Schwerte et al., 2006), it is possible that adrenergic activation of the cardiac β-adrenergic receptors may arise via circulating catecholamines. This leads to the secondary objective of this research; to examine whether loss of internal convection affects the hypoxic cardioreserpirstory responses in larval zebrafish.

3.2 MATERIALS AND METHODS

See Chapter 2 for details of fish care and breeding, morpholino micro-injections, phenotype confirmation and developmental matching.

3.2.1 Critical Partial Pressure of O_2 (P_{crit})

To measure O_2 consumption and asses critical PO_2 (P_{crit}), twelve 4 dpf larvae were pooled in a glass micro-respirometry chamber (2.94 ml volume; Loligo Systems, Tjele Denmark). Each chamber was equipped with a mini-magnetic stir bar, separated from the larvae by a stainless-steel mesh. The stir bar was set at 400 rpm by a mini-magnetic stir system (Loligo Systems, Tjele Denmar). Each chamber was filled with freshly-aerated system water, replaced and refilled 3 times to ensure complete homogeneity of gases throughout the mini-respirometry chamber. The entire system was submerged in a water bath, which was maintained at a constant 28.5$^{\circ}C$ or 34$^{\circ}C$ (experiment-dependent). There was also a small aquarium pump to ensure circulation in the water bath for an even temperature. Water PO_2 was monitored using fibre-optic O_2 electrodes (FOXY AL-300; Ocean Optics, Dunedin, FL, U.S.A.) and a laptop PC running the corresponding Ocean Optics Software. The electrodes were calibrated before each experimental trial using a zero O_2 solution containing 20 g/L of anhydrous sodium sulphite, after which the probes were transferred to aerated water (153 Torr). Water flow to the respirometer was stopped and the decline in chamber PO_2 was monitored over time to calculate O_2 consumption. The critical partial pressure of O_2 was calculated by graphing $\dot{M}O_2$ as a function of water PO_2, and subsequently determining the inflection point using 2 lines of best fit that maximize the combined R^2 values while still

retaining at least 5 $\dot{M}O_2$ data points for each line (Barrionuevo & Burggren, 1999). Separate P_{crit} trials were performed on 4 dpf sham and VEGF larvae at raised at 28.5°*C* and then acutely exposed to either 28.5°*C* or 34°*C* for the duration of the experiment. The 34°*C* exposure temperature was chosen as it was significant increase while still remaining well below the thermal max for larval zebrafish (Schaefer & Ryan, 2006) and within their natural range of temperatures (Engeszer et al., 2007).

3.2.2 Ventilation Frequency (f_V) and Heart Rate (f_H) Measurements

Larvae (4 or 5 dpf) were placed in a holding chamber and anaesthetised lightly using 0.06 mg ml^{-1} MS-222 solution; this way, fish continued to breathe but body movements were minimised. Larvae were provided continually with temperature-controlled water (28.5 °*C*) at a flow rate of 2 ml min^{-1}. Desired PO_2 was achieved using a Cameron Instruments GF3 (Cameron Instruments Inc., Guelph, ON, Canada) gas mixer by combining nitrogen and air, which was subsequently bubbled into the exposure water providing the holding chamber. Larvae were first exposed to a normoxic solution (153 Torr) for 5 min to obtain a baseline measure of f_V after which the flow was switched to hypoxic water (PO_2 = 55 Torr) for 30 min. Larvae were imaged for the duration of the experiment using a video camera (3CCD camera, Dage-MTI, USA) mounted to a dissecting microscope (SMZ1500, Nikon, Nikon SMZ 1500 microscope) (Nikon Instruments, Melville, NY, U.S.A.) and connected to a computer. Videos were captured using Debut Video Capture 2.25 open source, at 720 x 480 pixels and 30 frames s^{-1}. f_V was measured by counting opercular movements; f_H was determined by counting each heartbeat. Normoxic baseline was measured by averaging all counts over the entire 5 min exposure. During hypoxia, measurements were taken for 60 s every 5 min (for a total of 6 data points during hypoxia) and

the peak frequency was used for data analysis. Peak frequency was selected to best represent the maximal response possible and to account for the sporadic nature of larval ventilation.

A separate group of larvae were exposed to adrenaline instead of hypoxia. After baseline recording, fish were provided with a normoxic solution containing 10^{-4} M adrenaline bitartrate (containing 0.1g L^{-1} ascorbic acid). These concentrations were selected based on previous studies (Schwerte et al, 2006; Steele et al. 2009).

3.2.3 Immunohistochemistry

Larvae at 4 dpf were euthanized with MS-222, and subsequently fixed overnight at 4 *°C* in a phosphate-buffered saline solution (PBS) containing 4% paraformaldehyde (PFA). After fixation, the larvae were dehydrated in MeOH in a step-wise manner and stored at -80 *°C*. Prior to staining, the larvae were rehydrated in a step-wise manner and finally rinsed 3 times in 1X PBS containing 0.1% Tween-20 (PBST). The larvae were permeabilized in a blocking solution containing 0.8% Triton-X 100 and 3% bovine serum albumin dissolved in PBS and left for 1 h at room temperature. The primary antibody (antigen: 5-HT, dilution: 1:250, host: rabbit, source: Sigma) was added and the larvae were left on a mixer at 4 *°C* overnight. Larvae were rinsed 5X for 5 min intervals with PBST at room temperature. The secondary antibody (antigen: rabbit, wavelength: Alexa-488, dilution: 1:500, host: donkey, source: Thermo Fisher) was added to a solution containing 0.8% Triton-X 100 in PBST and incubated in the dark for 1 h at room temperature. Larvae were then rinsed 5X with PBST at room temperature and placed on a concave glass slide. A drop of 4',6-Diamidino-2-Phenylindole, Dihydrochloride (DAPI) 633 with ™Vectashield mounting medium was added and a coverslip was placed on top for imaging.

Images were taken using an Olympus confocal microscope (Olympus Scientific Solutions America, Waltham, MA, USA), with appropriate lasers for each fluorophore, and the images were processed using Olympus Zenblue software (Olympus Scientific Solutions America, Waltham, MA, USA).

3.2.4 Cell Counts

To determine NEC density, the larvae images were processed using Olympus Zenblue software (Olympus Scientific Solutions America, Waltham, MA, USA), and a 2D geometric shape was overlaid onto a region of the larvae. Three regions of measurements were chosen; i) the entire eye ii) the posterior-most section of the tail, and iii) the ventral region of the yolk sac. To account for proportional differences between larvae, the yolk sac and tail areas were determined by placing a rectangle on the area of interest and measuring 200 µm x Z µm, with Z being equal to 1/3 of the tail length (defined as the distance measured from the tip of the tail to the start of the yolk sac extension). The area was calculated for this region and the number of 5HT-positive cells were counted to determine the cell density. For the yolk sac, a rectangle of 200 µm x Z µm was overlaid as ventrally as possible without the corners falling off the edge of the yolk sac. For the eye, the whole eye was overlaid with either a circular or oval shape. For total NEC counts, all NECs on the visible side of the larval body were counted.

3.2.5 Statistical Analysis

All statistical analyses were performed using SigmaPlot (Version 12.2, SPSS Inc.). Data are presented as means ± 1 standard error of the mean (SEM). Results were analyzed using either Student's t-tests, 2-way analysis of variance (ANOVA) or 2-way repeated measures (RM)

ANOVA. All ANOVAs were followed by a Holm-Sidak post-hoc test when significant differences were detected. The significant limit for all analysis was 0.05

3.3 RESULTS

3.3.1 Interactions among Temperature, Resting Oxygen Consumption and Critical PO_2

Sham larvae and VEGF morphants both increased their rates of oxygen consumption ($\dot{M}O_2$) in response to an increase in ambient temperature of 5.5°*C* (Fig 3.2 A). Although, absolute increase in $\dot{M}O_2$ was greater in the sham larvae (32 μm/g/h) compared to the VEGF morphants (17 μm/g/h) the relative increases were approximately equal with a 46% increase for the sham larvae and a 48% increase for the VEGF morphants. At all temperatures, the VEGF morphants demonstrated a significantly lower $\dot{M}O_2$ compared to the sham larvae (Fig 3.2 A).

There was no significant difference in critical PO_2 (P_{crit}) between shams and VEGF morphants at 28.5°*C* (Figure 3.1 A; Fig 3.2 B). An increase in temperature to 34°*C* caused the P_{crit} of the VEGF morphants and sham larvae to increase significantly, although the sham larvae increased to a lesser extent. Consequently, the VEGF morphants at 34°*C* displayed a significantly higher P_{crit} than the 34°*C* sham counterparts (Fig 3.2 C).

3.3.3 Ventilation Responses to Hypoxia and Adrenaline

Shams and VEGF morphants at either 4 or 5 dpf exhibited similar resting ventilation frequencies (f_V; Fig 3.3 A-B). Upon exposure to hypoxia (55 Torr), sham larvae demonstrated a significant increase in f_V at 4 and 5 dpf (Fig 3.3 A-B). Hypoxia was without effect on f_V in the VEGF morphants at 4 dpf (Fig 3.3 A) but elicited a significant, albeit blunted hyperventilatory response at 5 dpf (Fig 3.3 B). Upon exposure to 10^{-4} M adrenaline, both the shams and the

VEGF morphants demonstrated a significant increase in f_V at 4 dpf (Fig 3.4 A). There was no difference between sham larvae and VEGF morphants in resting ventilation rates or peak hyperventilatory responses to 10^{-4} M adrenaline at 4 dpf (Fig 3.4 A).

3.3.4 Cardiac Responses to Hypoxia and Adrenaline

The VEGF morphants demonstrated a significantly lower resting heart rate (f_H) at 4 and 5 dpf compared to the sham larvae (Fig 3.3 C-D). Upon exposure to hypoxia, sham larvae underwent a significant increase in heart rate (f_H) at 4 and 5 dpf (Fig 3.3 C-D). In contrast, f_H in the VEGF morphants remained constant during hypoxia regardless of age (Fig 3.3 C-D). Consequently, the sham larvae demonstrated a significantly higher f_H in response to hypoxia compared to the VEGF morphants at 4 and 5 dpf (3.3 C-D). Upon exposure to 10^{-4} M adrenaline, 4 dpf sham larvae exhibited a significant increase in f_H. The VEGF morphants also experienced a significant increase in f_H at 4 dpf but the effect was blunted in comparison to the shams (Fig 3.4 B).

3.3.5 Neuroepithelial Cell Density and Distribution

Representative confocal microscopy images depicting the abundance 5-HT-positive NECs are shown for the head, yolk and tail regions (Fig 3.5). The VEGF morphants demonstrated significantly higher total counts of NECs when the entire side of a larvae was counted (Fig 3.6 A). The tail region demonstrated the lowest NEC density, the eye region had significantly higher NEC density than the tail region, and the yolk region had significantly higher NEC density than either the tail or the eye regions. The VEGF morphants also demonstrated

significantly higher NEC densities overall compared to the sham larvae. However, there were no regional effects on the differences in NEC density between shams and VEGF morphants (Figure 3.6 B).

3.4 FIGURES

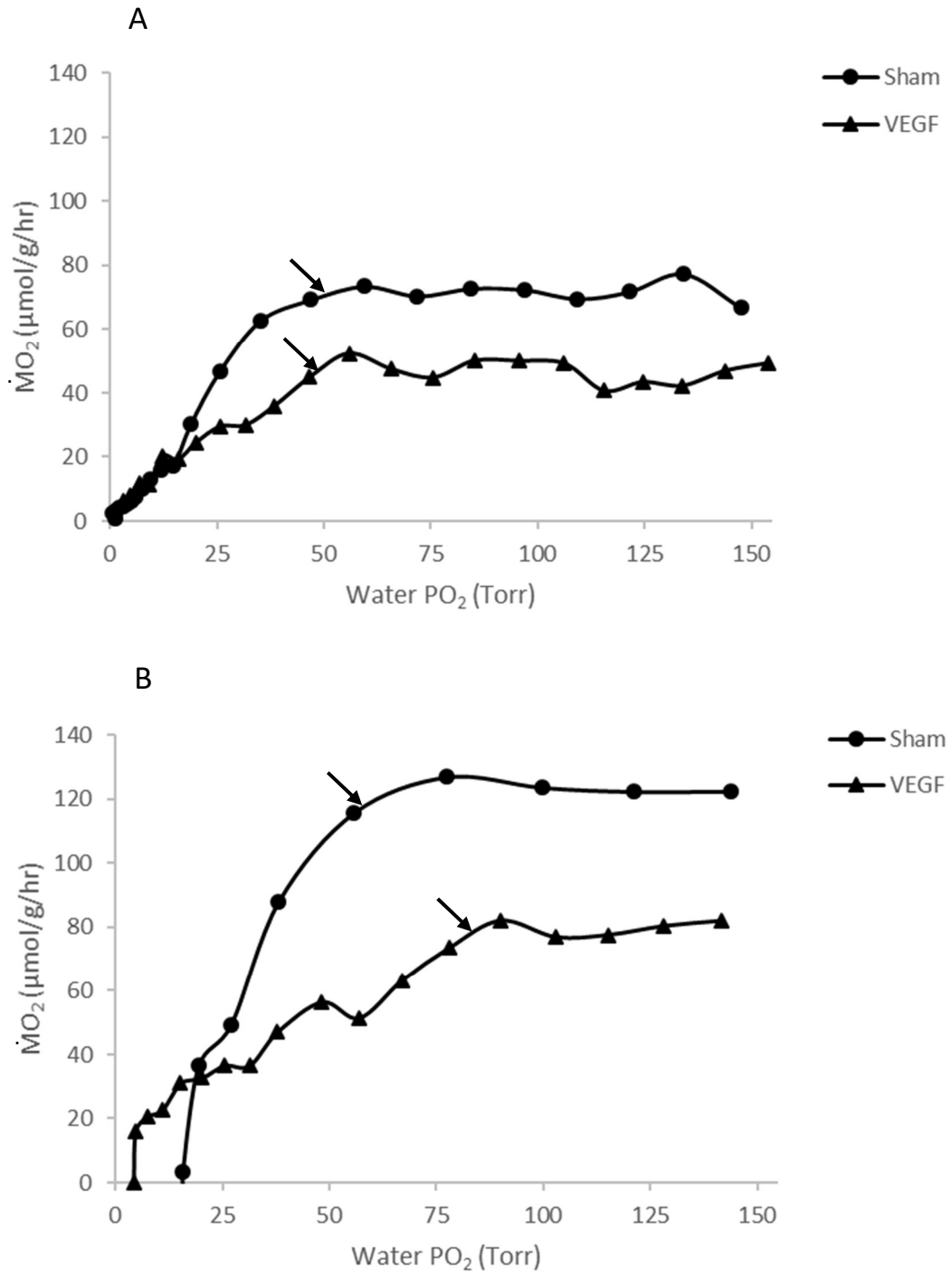

Figure 3.1 Representative critical PO_2 (P_{Crit}) traces for 4 dpf sham larvae and VEGF morphants at 28.5*°C* (A) and 34*°C* (B). P_{crit} indicated by arrow: 28.5*°C* sham 49 Torr, VEGF 46 Torr; 34*°C* sham 59 Torr, VEGF 83 Torr

Figure 3.2. $\dot{M}O_2$ (A) and critical P_{O_2} (B) for 4 dpf sham larvae and VEGF morphants at 28.5°C and 34°C. Values are shown as mean ± SEM. Letters indicate a significant difference between larval types and * indicates a significant difference between treatments. Greek letters indicate significant differences across temperatures, but not within larval types. Data were analyzed using a two-way ANOVA; $P < 0.05$. N = 7 – 13. For panel A the effect of larval type was $P < 0.001$, the effect of temperature was $P < 0.001$, larval type x temperature $P = 0.240$. For panel B the effect of larval type was $P = 0.068$, the effect of temperature was $P < 0.001$, larval type x temperature $P = 0.036$. Pairwise comparisons for: Temperature within sham $P = 0.030$, temperature within VEGF $P < 0.001$, larval type within 34°C $P = 0.012$, larval type within 28.5°C $P = 0.818$.

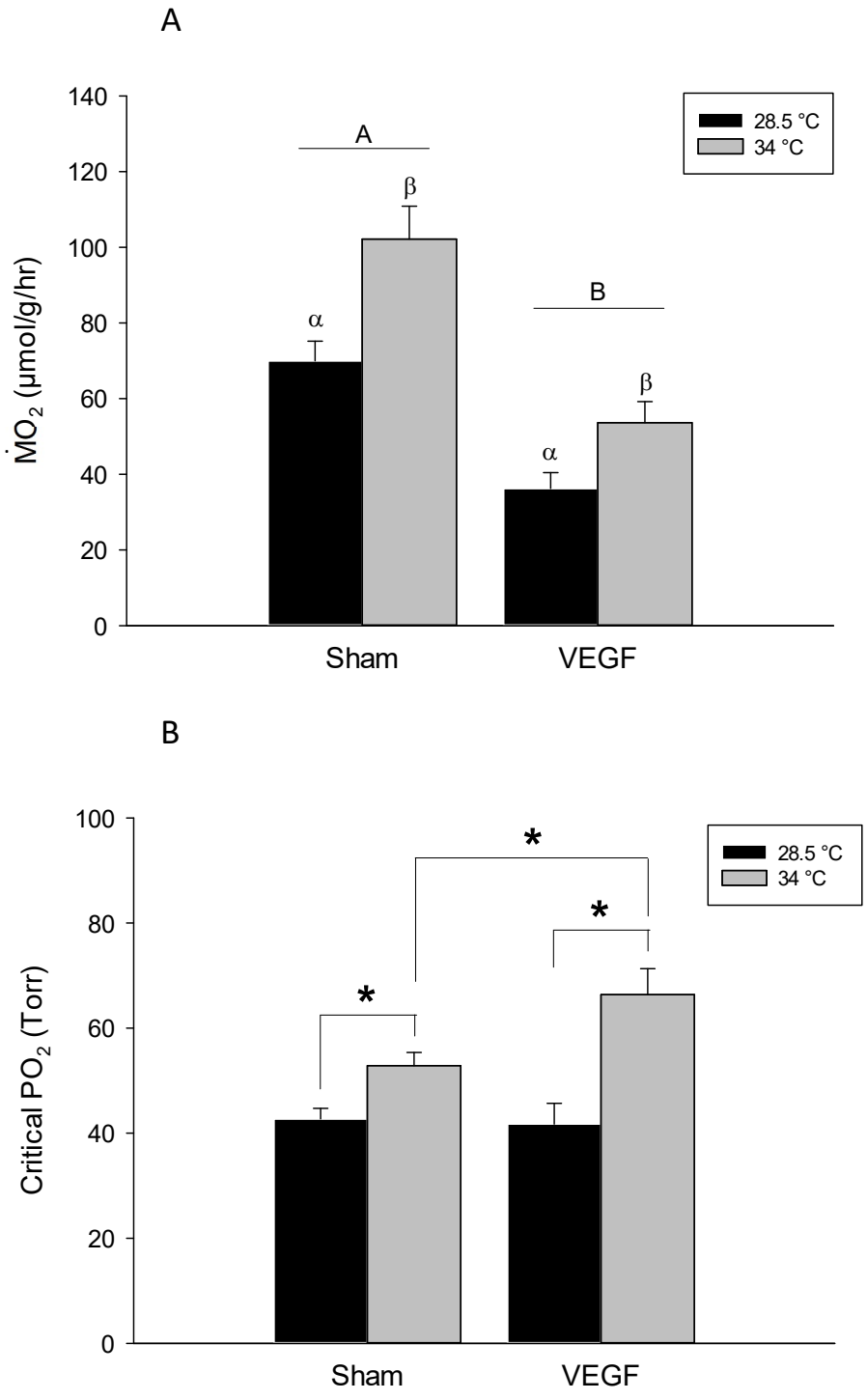
A
140
120
100
80
60
40
20
0
$\dot{M}O_2$ (µmol/g/hr)
28.5 °C
34 °C
A
B
α
β
α
β
Sham
VEGF
B
100
80
60
40
20
0
Critical PO_2 (Torr)
28.5 °C
34 °C
*
*
*
Sham
VEGF

Figure 3.3 Ventilation frequency (A,B) and heart rate (C,D) for sham and VEGF morphant larvae exposed to normoxia followed by hypoxia (55 Torr) while under light anaesthetic (0.06 mg ml^{-1} MS-222). The larvae used were either 4 dpf (A, C) or 5 dpf (B, D). * indicates a significant difference between treatments. Data were analyzed using a two-way RM ANOVA; $P < 0.05$. N = 7 – 13. For panel A the effect of treatment was $P < 0.001$, effect of larval type was $P = 0.050$, treatment x larval type $P = 0.002$. Comparisons within: sham for treatment $P < 0.001$, within VEGF for treatment $P = 0.172$, within normoxia for larval type $P = 0.874$, within hypoxia for larval type $P < 0.001$. For panel B the effect of treatment was $P < 0.001$, effect of larval type was $P = 0.002$, treatment x larval type $P < 0.001$. Comparisons within: sham for treatment $P < 0.001$, within VEGF for treatment $P = 0.010$, within normoxia for larval type $P = 0.540$, within hypoxia for larval type $P < 0.001$. For panel C the effect of treatment was $P < 0.001$, effect of larval type was $P < 0.001$, treatment x larval type $P = 0.030$. Comparisons within: sham for treatment $P < 0.001$, within VEGF for treatment $P = 0.055$, within normoxia for larval type $P < 0.001$, within hypoxia for larval type $P < 0.001$. For panel D the effect of treatment was $P < 0.001$, effect of larval type was $P < 0.001$, treatment x larval type $P = 0.002$. Comparisons within: sham for treatment $P < 0.001$, within VEGF for treatment $P = 0.082$, within normoxia for larval type $P = 0.002$, within hypoxia for larval type $P < 0.001$.

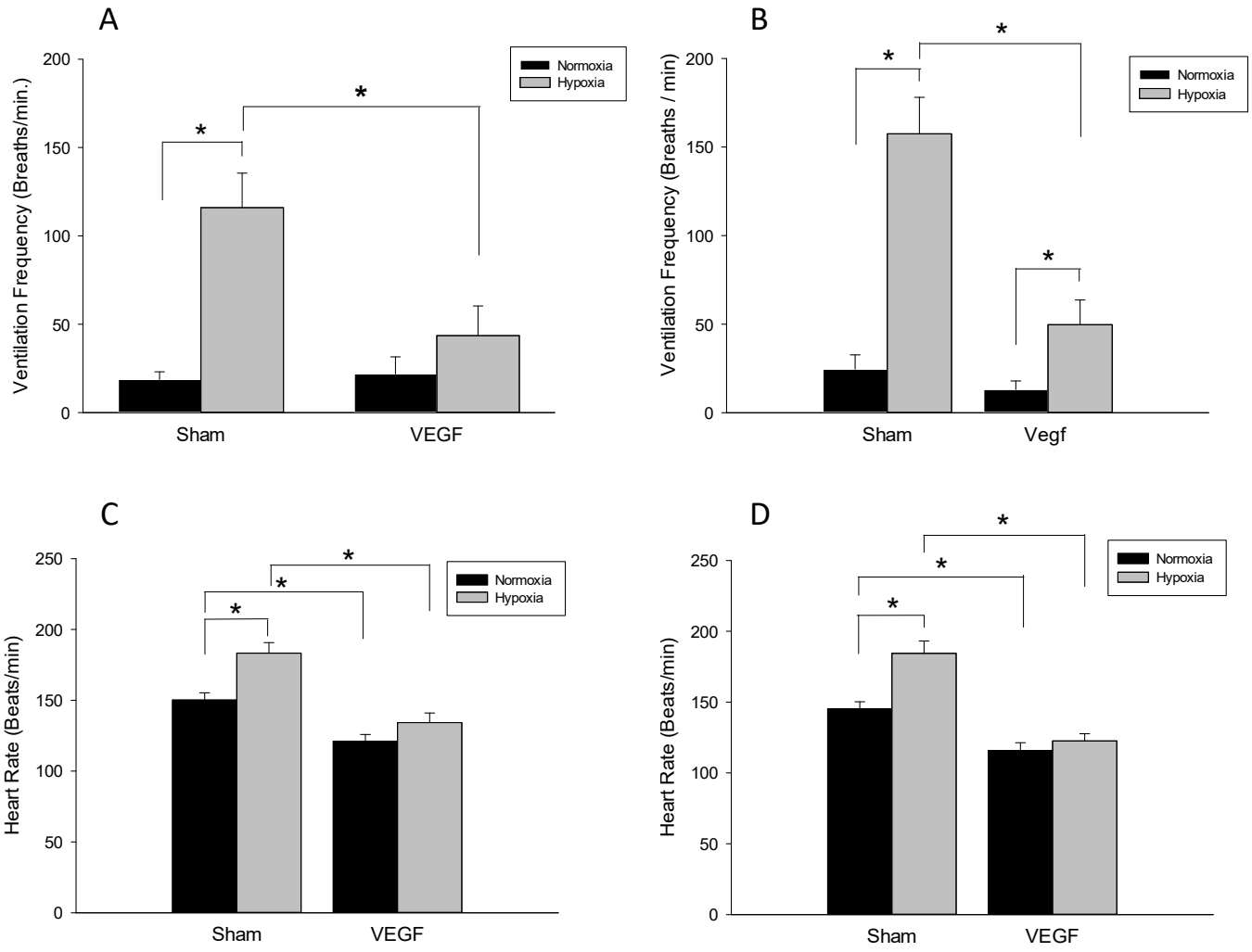
A
Ventilation Frequency (Breaths/min.)
200
150
100
50
0
Normoxia
Hypoxia
*
*
Sham
VEGF
B
Ventilation Frequency (Breaths / min)
200
150
100
50
0
Normoxia
Hypoxia
*
*
*
Sham
Vegf
C
Heart Rate (Beats/min)
250
200
150
100
50
0
Normoxia
Hypoxia
*
*
*
Sham
VEGF
D
Heart Rate (Beats/min)
250
200
150
100
50
0
Normoxia
Hypoxia
*
*
*
Sham
VEGF

Figure 3.4 Ventilation frequency (A) and heart rate (B, C) for 4 dpf sham larvae and VEGF morphants exposed to control anesthetic solution (0.06 mg ml^{-1} MS-222) followed by the same anaesthetic solution containing 10^{-4} M adrenaline bitartrate. Letters indicate a significant effect of treatment. An * indicates a significant difference between treatments. Data were analyzed using a two-way RM ANOVA (A, B) or Student's t-test (C); $P < 0.05$. N = 12 – 15. For panel A the effect of treatment was $P = 0.004$, effect of larval type was $P = 0.508$, treatment x larval type $P = 0.734$. For panel B the effect of treatment was $P < 0.001$, effect of larval type was $P = 0.003$, treatment x larval type $P < 0.001$. Comparisons within: sham for treatment $P < 0.001$, VEGF for treatment $P < 0.001$, control for larval type $P = 0.022$, adrenaline for larval type $P < 0.001$. For Panel C the effect of larval type was $P = 0.001$.

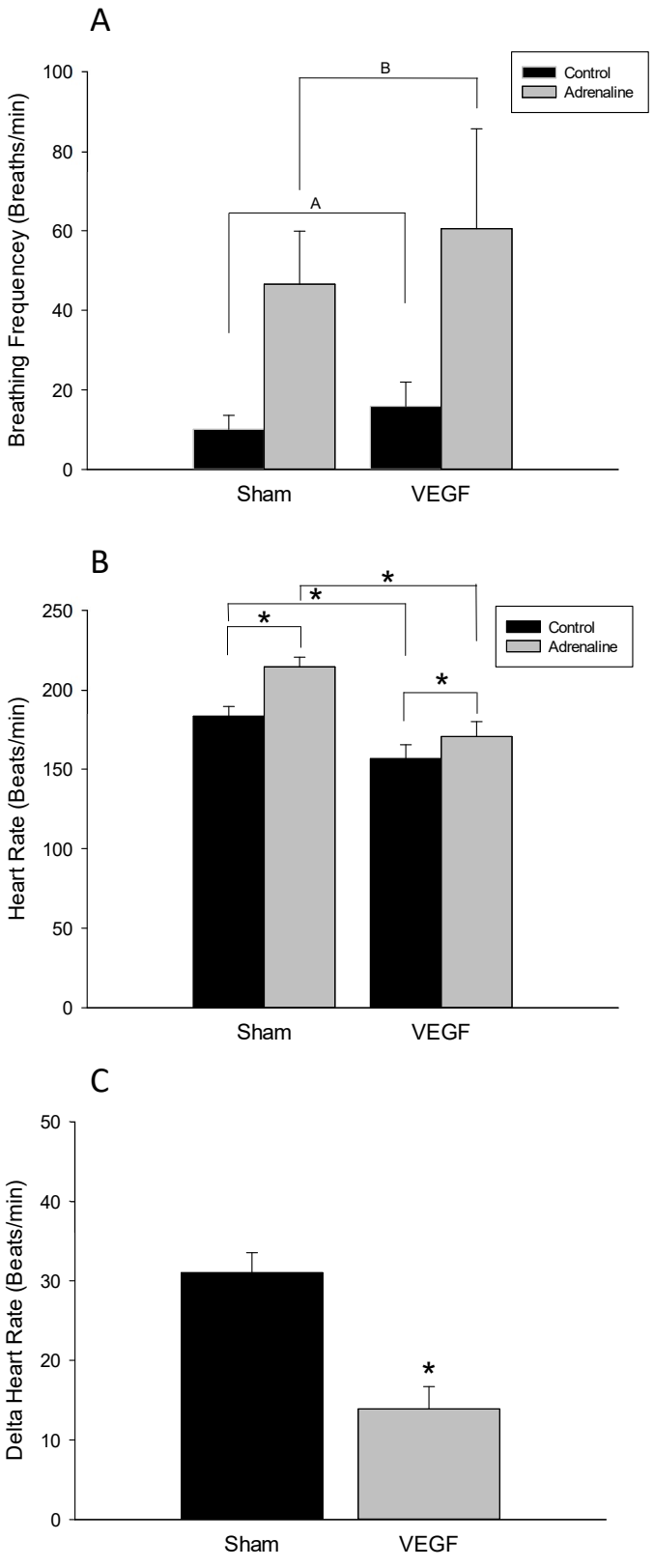
A
Breathing Frequencey (Breaths/min)
100
80
60
40
20
0
B
A
Control
Adrenaline
Sham
VEGF
B
Heart Rate (Beats/min)
250
200
150
100
50
0
*
*
*
*
Control
Adrenaline
Sham
VEGF
C
Delta Heart Rate (Beats/min)
50
40
30
20
10
0
*
Sham
VEGF

Figure 3.5 Distribution of NECs in sham larvae (A, C, E) and VEGF morphants (B, D, F) in 3 locations at 4 dpf. Specimens were immunolabelled for serotonin (green) and stained with DAPI, a nuclear stain (blue). The locations examined are as follows head (A, B), yolk (C, D) and tail (E, F).

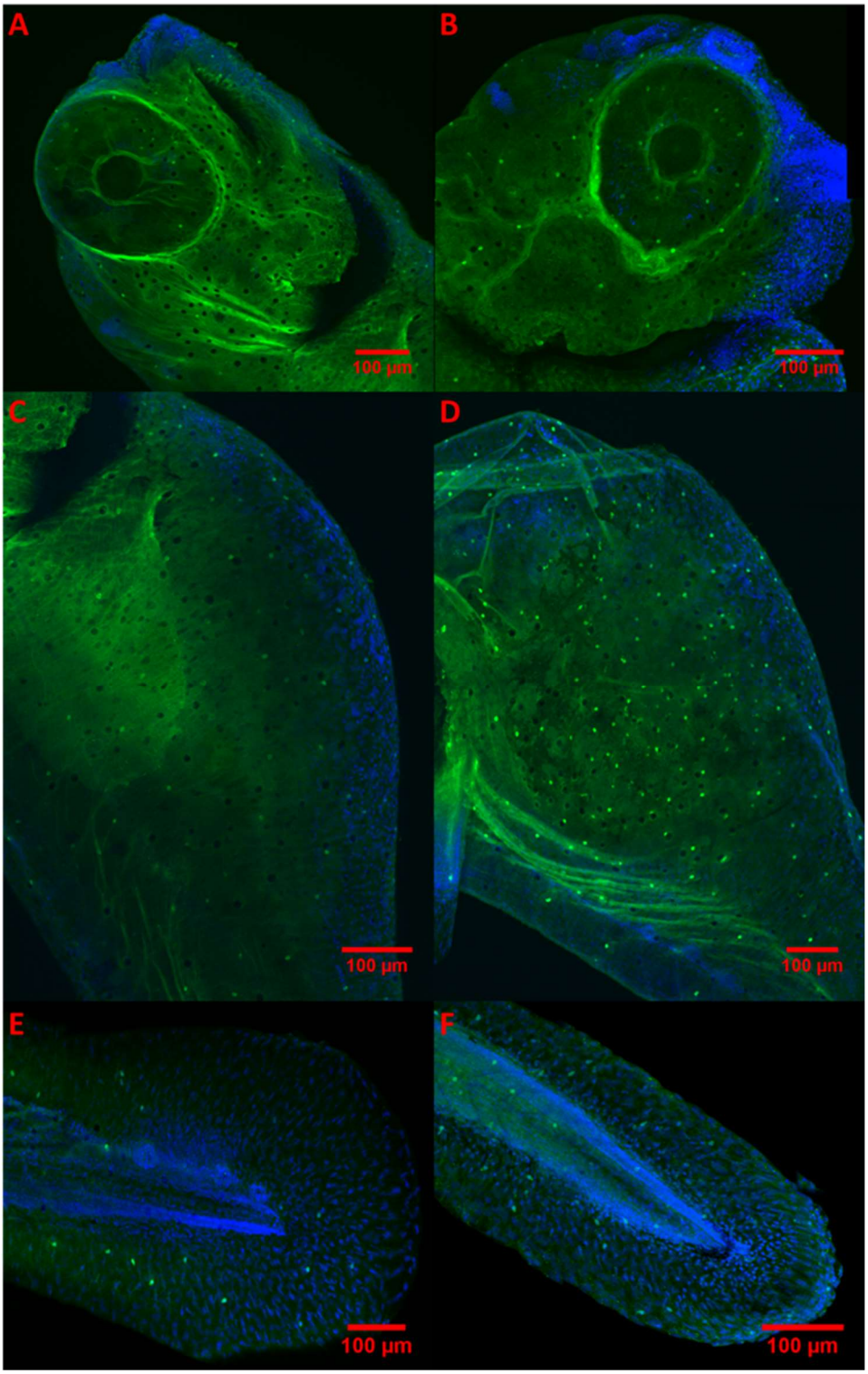
A
100 µm
B
100 µm
C
100 µm
D
100 µm
E
100 µm
F
100 µm

Figure 3.6 NEC count and regional density in shams or VEGF morphants for at 4 dpf. Total NEC counts (A) are shown for a single side of the larvae. Regional NEC density (B) was determined for 3 locations, eye, tail and yolk. * indicates a significant difference between groups. Letters indicate a significant difference between regions. A t-test was used to analyze panel A, and a two-way ANOVA was used in panel B; $P < 0.05$. N = 8 – 12. For panel A the effect of larval type was $P < 0.001$. For Panel B the effect of larval type was $P = 0.001$, the effect of region was $P < 0.001$ and larval type x region $P = 0.695$.

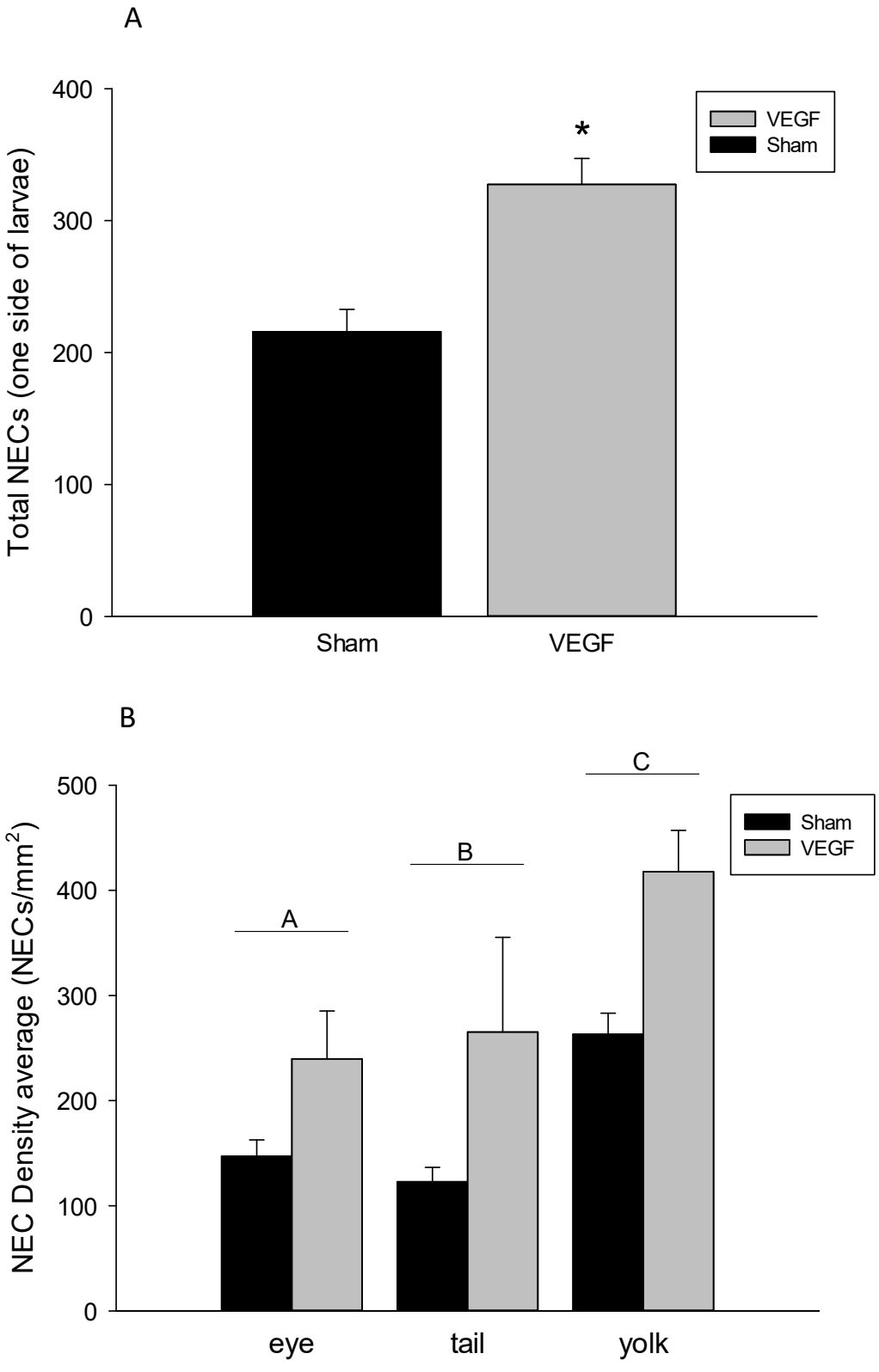
A
400
300
200
100
0
Total NECs (one side of larvae)
*
VEGF
Sham
Sham
VEGF
B
500
400
300
200
100
0
NEC Density average (NECs/mm2)
A
B
C
Sham
VEGF
eye
tail
yolk

3.5 DISCUSSION

Internal convection is critically involved in sustaining normal rates of gas transfer in zebrafish larvae (Chapter 2). Thus, I reasoned that hypoxia performance would be impaired in developing larvae lacking functional blood circulation, especially in fish experiencing an increased O_2 demand associated with exposure to higher temperatures. However, despite the absence of the usual hypoxic hyperventilation and tachycardia responses, the fish lacking internal convection and kept at standard husbandry temperature (28.5^oC) did not exhibit an obvious impairment of performance, at least as indicated by similar P_{crit} values. However, when experiencing an increase in aerobic metabolic rate associated with acclimation to 34^oC, the larvae without functional circulation exhibited an increase in P_{crit}, which is indicative of a decline in hypoxia performance.

3.5.1 Internal Convection and Hypoxia Performance

Although the results of previous studies demonstrated that functional ablation of hemoglobin does not affect resting O_2 uptake in larval zebrafish (Jacob et al., 2002; Rombough & Drader, 2009), the current results (in agreement with the results of Chapter 2), clearly indicate that diffusion alone, is inadequate to sustain normal rates of O_2 uptake. These findings reinforce a major take-home message of this thesis (see Chapter 2) that the insensitivity of zebrafish larvae to elimination of haemoglobin cannot provide evidence that convection, *per se*, is unrequired for O_2 uptake in these developing fish.

As environmental PO_2 decreases, the trans-cutaneous PO_2 gradient must shrink and thus constrain the rate of O_2 uptake. In fish with an intact circulatory system, the rate at which the

PO_2 diffusion gradient declines is regulated, in part, by the convective removal of O_2 as it enters the fish as well as its binding to haemoglobin. Eventually an environmental PO_2 (P_{crit}) is reached at which point O_2 uptake can no longer sustain normal rates of aerobic metabolism.

Given the loss of convection resulted in a significant reduction in the rate of resting O_2 consumption (Chapter 2, Fig. 3.2 A), it was predicted that the ability to extract O_2 from the environment under hypoxic conditions would be hindered. As in previous studies (Barrionuevo & Burggren, 1998; C. E. Robertson et al., 2014), the P_{crit} was used as a metric to assess O_2 extraction capacities during progressive hypoxia. Under normal acclimation (28.5 *°C*) conditions, P_{crit} was unaffected in the VEGF morphants. The ability of fish, regardless of convection status, to maintain constant rates of O_2 uptake during progressive hypoxia until a similar PO_2 threshold is reached, at a first glance, is seemingly at odds with the reduced resting rates of O_2 consumption in the VEGF morphants lacking internal convection. The most likely explanation for the lack of any difference in P_{crit} between the larvae with and without convection is that resting aerobic metabolic rate was suppressed to a lower resting level as a compensatory effort to match the lowered capacity for O_2 uptake. Thus, even without convection serving to sustain PO_2 diffusion gradients, the VEGF morphants were able to sustain their lower rates of metabolism for as long as the shams with their higher rates of metabolism.

Increasing ambient temperature presented a method to force an increase in resting O_2 consumption in the VEGF morphants (Fig 3.2 A). Both larval types responded to a 5.5 *°C* increase in temperature with comparative relative increases in $\dot{M}O_2$ with a 46% increase in the sham larvae and a 48% increase in the VEGF morphants (Fig 3.2 A). Thus, despite having different

absolute increases in $\dot{M}O_2$ both larval types demonstrate similar relative increases in MO_2 with respect to their resting $\dot{M}O_2$ at the lower ambient temperature.

At 34*℃*, the sham larvae demonstrated the capacity to adjust their extraction ability to the increased O_2 demand with no significant change in critical PO_2. The VEGF morphants, however, did not display this capacity to adjust their extraction capabilities any further, which resulted in a significant increase in P_{crit} (Fig 3.2 C).

Interestingly, the 5.5*℃* increase caused the VEGF morphants to have a resting O_2 consumption rate that was equal to that of the sham larvae at 28.5*℃* (Fig 3.2 B). By matching the resting rates of O_2 consumption, the VEGF at 34*℃* have a similar O_2 demand as the sham larvae do at 28.5*℃*, making for a clearer assessment of the impact of internal convection on environmental O_2 extraction capacity, independent of metabolic rate. When resting $\dot{M}O_2$'s are matched, internal convection clearly has a beneficial impact on the O_2 extraction abilities of larval zebrafish under hypoxic conditions as demonstrated by the significantly higher P_{crit} of the 34*℃* VEGF morphants relative to the 28.5*℃* sham larvae (Fig 3.2 D).

3.5.2 Internal Convection and the Hypoxic Cardiorespiratory Responses

In larval zebrafish, internal convection not only improves O_2 extraction capacities, but it also appears to play an important role in permitting the usual hypoxic cardiorespiratory responses. Internal convection may be directly involved in mediating these responses or indirectly involved through secondary roles associated with normal tissue development. Typically, upon exposure to hypoxic conditions, larval zebrafish demonstrate an increase in f_V (Jonz & Nurse, 2005). The loss of internal convection, however, either prevented (at 4 dpf) or

blunted (at 5 dpf) the hyperventilatory responses to hypoxia. The appearance of this (blunted) response in the VEGF morphants at 5 dpf is likely a consequence of the overall greater magnitude of the response at 5 dpf compared to 4 dpf, which was observed in both larval types. It would appear however, that internal convection is not a physical prerequisite for ventilation to increase because the VEGF morphants, despite their lack of internal convection, demonstrated an increase in f_V in response to exogenous adrenaline that was equivalent to the response in the sham larvae.

To explore the underlying cause for the absence of a hypoxic hyperventilatory response in the VEGF morphants lacking convection, the number of skin NECs was determined in the larvae at 4 dpf using immunohistochemical staining. The VEGF morphants not only demonstrated the presence of NECs but they exhibited significantly higher absolute numbers across the entire larvae when compared to shams (Fig 3.5, Fig 3.6 A). These findings suggest that development of the chemosensory NECs themselves can occur independently of internal convection and that the absence of hyperventilation in the VEGF morphants cannot be explained by decreased numbers of chemosensory NECs.

Larval zebrafish develop cutaneous NECs at 24 hpf, which peak in number at 3 dpf and then decrease from this point onwards (Coccimiglio & Jonz, 2012). It has been demonstrated, however, that a short 24 h exposure to severe hypoxia (30 Torr) at 24 hpf resulted in retention of the cutaneous NECs (Coccimiglio & Jonz, 2012; Dean et al., 2017). This retention of NECs in larval zebrafish is thought to be associated with their increased mitogenic activity upon exposure to hypoxia (Dean et al., 2017). Similar mitogenic effects of hypoxia were reported for carotid bodies of mammals, yielding glomus cell proliferation and organ hypertrophy with

prolonged exposure (Nurse & Vollmer, 1997; Pardal et al., 2007; Platero-Luengo et al., 2014). The glomus (Type II) cells of the carotid body are considered to be the homologous mammalian counterpart to the NECs (Jonz & Nurse, 2006). With this in mind, the lack of internal convection may have been accompanied by persistent internal hypoxia in the VEGF morphants, which in turn, may have led to the increased numbers of NECs.

In addition to an increase in f_V, larval zebrafish exhibit an increase in f_H in response to acute hypoxia (Fig 3.3; Barrionuevo & Burggren, 1999; Jacob et al., 2002; Jonz & Nurse, 2005; Perry et al., 2009) which, based on the results of the current study, is apparently dependent on an intact circulatory system. As discussed above for the ventilation responses, the absence of tachycardia in the VEGF morphants cannot be explained by fewer numbers of NECs. Unlike the ventilatory response, the cardiac response to exogenous adrenaline was significantly reduced in the VEGF morphants at 4 dpf (Fig 3.4 B, C). The reason for the cardiac adrenergic insensitivity is unclear; however, the hearts of the VEGF morphants appeared underdeveloped. In turn, the cardiac underdevelopment may have been related to a lack of proper sheer stresses in the heart which are important for cardiac development in larval zebrafish (Hierck et al., 2008). On the other hand, the VEGF morphants may simply be less sensitive to adrenaline owing to improper development of cardiac β-receptors.

3.5.3 Conclusions

In the absence of internal convection, larval zebrafish at 4 dpf do not experience hypoxic hyperventilation or tachycardia, which are typically observed in intact larvae at 28.5^oC (Barrionuevo & Burggren, 1999; Jacob et al., 2002; Jonz & Nurse, 2005; Perry et al., 2009).

Despite the lack of circulation and routine cardiorespiratory responses, hypoxia performance appeared to be unaltered in the VEGF morphants based on an unchanged P_{crit}. The constancy of P_{crit} in the fish with and without convection may reflect the lowered resting $\dot{M}O_2$ in the VEGF morphants. In support of this idea, when acclimation temperature was increased in the VEGF morphants to match metabolic rate with the shams at 28.5^oC, the P_{crit} was markedly lower in the morphants.

During early larval stages, zebrafish rely predominantly on their skin and not their gills for respiratory gas transfer. Because the gills are not yet developed, the physiological significance of hypoxic hyperventilation is unclear. The increased movement of water through the opercular cavities may increase flow over the skin and thus disrupt external boundary layers adjacent to the skin. However, even if hyperventilation disrupts external boundary layers near the skin it is unclear whether the associated increased energetic cost of ventilation is offset by any improvement in O_2 extraction.

Most adult fish, including zebrafish, respond to hypoxia with bradycardia in (Randall, 1982). In terms of heartrate, larval zebrafish demonstrate the opposite effect, increasing heart rate under hypoxic conditions however, they also demonstrate an increase in cardiac output similar to what is observed in many adult fish (Jacob et al., 2002; Randall, 1982; C. Wood & Shelton, 1980). Although this unique larval response is likely due to a lack of vagal innervation at this stage in development, my findings suggest a potentially beneficial role for increased internal convection. This increase in heartrate and cardiac output may help compensate for the reduction in the PO_2 gradient between the tissues and the external environment that occurs during environmental hypoxia.

CHAPTER 4

General Discussion

4.1 Resting O_2 Consumption and Hypoxic Compensatory Mechanisms

O_2 supply is essential to the survival of aerobic tissues. Prolonged periods of hypoxia in these tissues can lead to insufficient ATP supply, causing loss of ionic and osmotic equilibria, excessive calcium release and ultimately cell necrosis (Hochachka, 1986). To avoid these damaging effects of hypoxia, organisms may employ compensatory mechanisms to ensure that O_2 demand does not exceed the O_2 supply. In larval zebrafish, I showed that internal convection has a significant impact on resting aerobic metabolic rate, namely O_2 uptake ($\dot{M}O_2$) and CO_2 excretion ($\dot{M}CO_2$) (Chapter 2). It is interesting to note, however, that when acutely stopping internal convection using anaesthetic, the rates of skin boundary layer O_2 flux decreased to a greater extent than what was observed for whole body $\dot{M}O_2$ in larvae that had developed entirely without internal convection. These results suggest that while developing without internal convection, the VEGF morphants were able to compensate to improve their ability to extract O_2 in the absence of convective O_2 transport.

Chronic hypoxia exposure can induce a variety of compensatory mechanisms in larval zebrafish during hypoxia exposure ranging from structural adaptations, such as increased blood perfusion and blood vessel size (Moore et al., 2006; Schwerte et al., 2003), increased numbers of skin NECs (Dean et al., 2017) and altered gene regulation for key metabolic pathways (C. E. Robertson et al., 2014; Ton et al., 2003). The increase in NEC density observed in the VEGF morphants suggests that these fish were experiencing chronic internal hypoxia. C. E. Robertson et al. (2014) found that prior exposure to either hypoxia or anoxia in larval zebrafish resulted in improved hypoxia performance at 4 dpf. Thus, larvae pre-exposed to either hypoxia or anoxia showed similar increases in resting $\dot{M}O_2$ compared to control larvae re-exposed to hypoxia, and

were able to maintain uptake at significantly lower levels of O_2. These results indicate that hypoxia exposure during development has a beneficial effect on overall hypoxia performance in later larval stages and supports the idea that the VEGF morphants are experiencing chronic internal hypoxia during development owing to their lack of convective O_2 transport.

Although the exact mechanisms underlying the compensatory adjustments accompanying loss of internal convection are currently unknown in larval zebrafish, one possibility is a reduction of barriers that impede passive O_2 diffusion. In bullfrog tadpoles exposed to hypoxia, the skin epithelium undergoes a reduction in thickness concurrently with increased capillarity (W. W. Burggren & Mwalukoma, 1983). This reduced epithelium thickness reduces the barrier impeding passive O_2 diffusion, improving O_2 uptake. A similar mechanism, if occurring in larval zebrafish, could be contributing to sustaining $\dot{M}O_2$ in the VEGF morphants in comparison to larvae acutely experiencing a cessation of blood flow.

Another adaptive mechanism that animals may exhibit in the face of hypoxia exposure is metabolic suppression to decrease their overall rates of ATP turnover (Hochachka & Lutz, 2001). Metabolic suppression can be achieved through multiple mechanisms including decreased ion pumping via channel arrest and overall reductions in protein synthesis (Dalla Via et al., 1994; Hochachka & Lutz, 2001). Zebrafish larvae may adhere to this trend because hypoxic exposure resulted in a significant reduction in the expression of genes encoding contractile, extracellular matrix and cytoskeletal proteins (Ton et al., 2003). Because these motility and cell structure proteins are highly abundant, their suppression likely represents an important energy saving strategy in larval zebrafish. The downregulation of these motility proteins as an energy saving strategy to compensate for reduced O_2 uptake capacity may partly

explain the reduced motility observed in the VEGF morphants. Given that they are less capable of suppling O_2 to their internal tissues, the VEGF morphants must manage with a reduced maximum rate of O_2 supply. As such, they presumably re-allocate their overall energy budget to minimize non-essential ATP-consuming activities. Similar behavioural strategies were observed in rainbow trout (*Oncorhynchus mykiss*) where reduced motility was correlated with improved survival rates during prolonged hypoxia exposures (van Raaij et al., 1996).

Hypoxia inducible factor (HIF-1 α) is a master regulator of cellular and developmental homeostasis during hypoxia exposure (Benita et al., 2009; Iyer et al., 1997). The protein in its active form is part of a dimeric complex with HIF-1 β, which is stabilized in the presence of low O_2. In zebrafish larvae, increases in HIF-1 α expression have been correlated with improved hypoxia performance (C. E. Robertson et al., 2014). The HIF-1 α protein has also been found to promote the expression of insulin-like growth factor-binding protein (IGFBP)- a protein that binds and inhibits various effects of insulin like growth factor (IGF) 1 and 2 (Kajimura et al., 2005, 2006; Kamei et al., 2008). IGF promotes a wide range of anabolic activity in teleosts, including tissue growth and increased intermediary metabolism (A. W. Wood et al., 2005). Therefore, it is possible that some of the hypo-metabolic characteristics observed in the VEGF morphants are in part being mediated by the effects of HIF-1 α on IGFBP. Because loss of internal convection decreases O_2 extraction capacity, resulting in insufficient O_2 supply to the internal tissues deep within the larva, it is likely that through the effects of HIF-1 α and other hypoxia related factors, the VEGF morphants are modulating rates of ATP turnover and O_2 consumption in their tissues. Reduction of O_2 consumption in the outer tissues would better allow the limited O_2 being absorbed to be spared for delivery to the tissues deep within the

organism. This would benefit the internal tissues and likely reduce the occurrence of damaging anoxia deep within the organism. This modulation of resting aerobic metabolic rate in certain tissues is likely an active compensation in an attempt to optimize the limited O_2 supply provided solely by diffusive means.

Interestingly, although the VEGF morphants demonstrated a reduced resting metabolic rate, an increase in environmental temperature led to a rise in O_2 consumption. Given that O_2 consumption already was significantly constrained in the VEGF morphants, these results beg the question as to how $\dot{M}O_2$ was able to increase further as temperature was elevated. A portion, but not all, of the increase can be attributed to the increase in the rate of O_2 diffusion associated with increasing temperature. Given that the Q10 for O_2 diffusion is ~ 1.3, we would expect an approximate 16.5% increase in the rate of O_2 diffusion for a 5.5*°C* increase in temperature. The VEGF morphants, however, increased their rate of O_2 consumption by ~40%, and as such cannot be explained by the thermal effects on simple diffusion, alone. It is possible that owing to the prolonged hypoxia exposure, the VEGF morphants are overcompensating their hypoxic hypometabolism, overshooting the O_2 restrictions imposed by relying on purely diffusive O_2 supply. Increasing ambient temperature may effectively 'bypass' many of the regulatory mechanisms imposed by HIF-1 α, and therefore allow an increase in resting metabolic rate.

4.2 Unanswered Questions and Future Directions

Although net O_2 consumption and regional O_2 flux rates were determined, it is still unclear where the precise locations of O_2 consumption are or how these sites of consumption change in the face of hypoxia. Recently, a novel technique was described that uses microspheres filled with an O_2 sensitive ratiometric dye to measure O_2 levels in the GI tracts of insects (A. B. Robertson, 2017). Use of these spheres combined with our micro-sphere injection technique (Chapter 2), could allow direct real-time visualization of internal PO_2 in larval zebrafish. In this way, we could observe not only how internal PO_2 differs spatially within the organism, but also how changes such as external hypoxia or loss of convection may affect internal O_2 status. This technique also could be utilized to directly observe the impact of internal convection, the compensatory effects of prior hypoxia exposure and the tachycardia and hyperventilatory hypoxic responses on internal PO_2 in larval zebrafish.

Our findings also suggested indirectly that larval zebrafish might be able to modify their epithelial thickness as an adaptive response to hypoxia exposure. It would be interesting to examine epithelial thickness in larval zebrafish after various levels and lengths of hypoxia exposure, as it may present a previously unknown adaptive hypoxia response in larval teleosts. The gills of adult teleosts are considered to be highly plastic organs, able to adapt both their size and perfusion in response to O_2 demands and ionic challenges (Henriksson et al., 2008; Sollid & Nilsson, 2006). Some species may adjust branchial epithelial thickness in response to O_2 availability (Henriksson et al., 2008; Tuurala et al., 2005) and other environmental challenges such as softwater or metal exposure (Lappivaara et al., 1995; Leino & McCormick, 1993; McCormick et al., 1989), suggesting that this may be a common adaptive mechanism in

teleosts. To date, the possibility of a similar adaptive mechanism has not been examined in teleost larvae, but given that the larval epithelium is often considered the respiratory equivalent of the gill epithelium and that similar effects have been observed in bullfrog tadpoles (W. W. Burggren & Mwalukoma, 1983), it is possible that a similar strategy may also be used by larval zebrafish.

4.3 Summary and Significance of Thesis

This thesis broadens our understanding of one of the most critical systems in vertebrates, internal convection. Convective O_2 transport is necessary for the maintenance of O_2 supply in large adult vertebrate species. Studying the impact of internal convection in smaller, but similarly complex organisms illustrates the limits of purely diffusive O_2 supply. Understanding the limits for O_2 diffusion in a small complex organism sheds light on the role of internal convection in these organisms and on the developmental pressures placed upon the cardiovascular system. Ultimately, understanding the fundamental mechanisms that organisms use to survive, and the limits of these systems, is a key theme in the field of comparative physiology.

The overall objective of my thesis was to understand the role of internal convection on O_2 uptake in a small, but complex organism, the larval zebrafish. Through this work, I provided insights on the impacts of internal convection on the development of the O_2 sensing NECs and the mediation of the various hypoxia responses.

In chapter 2, I demonstrated that internal convection is paramount for maintaining resting O_2 consumption and aerobic metabolic rate in larvae at 4 dpf. Based on the

respirometry and SMOT experiments, I concluded that these reductions are due to an inability to supply sufficient O_2 to the metabolizing tissues deep within the organism, resulting in the collapse of the internal PO_2 gradients. Overall, even under normoxic conditions, it appears that convective O_2 transport is required to maintain resting rates of O_2 consumption in larval zebrafish both throughout development and acutely.

In Chapter 3, I further explored the implications of internal convection on the ability of larval zebrafish to extract O_2 from the environment under hypoxic conditions. The results of that study indicated that internal convection plays an important role in augmenting the ability of larvae to maintain a given rate of O_2 uptake in the face of decreasing environmental O_2. With intact internal convection, larval zebrafish were better able to defend a constant aerobic metabolic rate in the face of declining environmentally available O_2. The results also demonstrated that internal convection plays an important role in mediating the hypoxic hyperventilatory and tachycardia responses, although the underlying mechanisms remain unclear. I also characterized the spatial distribution and density of epithelial NECs in larval zebrafish, and demonstrated that internal convection affects overall NEC number, but not relative spatial distribution. These findings indicate that in larval zebrafish, the NECs are fully capable of developing in the absence of internal convection.

4.4. Concluding Remarks

The results of this thesis demonstrate that in larval zebrafish, convective O_2 transport is required to maintain sufficient O_2 supply, and that resting O_2 demands cannot be met solely by passive diffusion. The data also demonstrated that internal convection has a beneficial effect

on overall hypoxia performance in zebrafish larvae by improving O_2 extraction capacities in the face of environmental hypoxia. Lastly, I demonstrated a potential role of internal convection in mediating the cardiorespiratory responses to hypoxia, one that is independent of the development, presence and quantity of epithelial NECs.

BIBLIOGRAPHY

Bakkers, J. (2011). Zebrafish as a model to study cardiac development and hman cardiac disease. *Cardiovascular Research, 91*(2), 279-288. doi: https://doi.org/10.1093/cvr/cvr098

Barrionuevo, W. R., & Burggren, W. W. (1998). O2 consumption and heart rate in developing zebrafish (*Danio Rerio*): influence of temperature and ambient O2. *Metabolism And Heart Rate In Developing Zebrafish*, R505-R513.

Barrionuevo, W. R., & Burggren, W. W. (1999). O2 consumption and heart rate in developing zebrafish (*Danio Rerio*): influence of temperature and ambient O2. *Metabolism And Heart Rate In Developing Zebrafish*, R505-R513.

Barrionuevo, W. R., Fernandes, M. N., & Rocha, O. (2009). Aerobic and anaerobic metabolism for the zebrafish, *Danio rerio*, reared under normoxic and hypoxic conditions and exposed to acute hypoxia during development. *Brazilian Journal of Biology, 70*(2), 425-434.

Benita, Y., Kikuchi, H., Smith, A. D., Zhang, M. Q., Chung, D. C., & Xavier, R. J. (2009). An integrative genomics approach identifies Hypoxia Inducible Factor-1 (HIF-1)-target genes that form the core response to hypoxia. *Nucleic Acids Research, 37*(14), 4587-4602. doi: 10.1093/nar/gkp425

Boutilier, R. G., Heming, T. A., & Iwama, G. K. (1984). Physiochemical Parameters for Use in Fish Respiratory Physiology. *Fish Physiology, XA*, 403-430.

Burggren, & Pinder, A. (1991). Ontogeny of Cardiovascular and Respiratory Physiology in Lower Vertebrates. *Annual Reviews: Physiology, 53*, 107-135.

Burggren, W. W., & Mwalukoma, A. (1983). Respiration During Chronic Hypoxia And Hyperoxia In Larval And Adult Bullfrogs (*Rana Catesbeiana*). *The Journal of Experimental Biology, 105*, 191-203.

Chow, D. C., Wenning, L. A., Miller, W. M., & Papoutsakis, E. T. (2001a). Modeling pO2 Distributions in the Bone Marrow Hematopoietic Compartment. I. Krogh's Model. *Biophysical Journal, 81*(2), 675-684. doi: https://doi.org/10.1016/S0006-3495(01)75732-3

Chow, D. C., Wenning, L. A., Miller, W. M., & Papoutsakis, E. T. (2001b). Modeling pO2 Distributions in the Bone Marrow Hematopoietic Compartment. II. Modified Kroghian Models. *Biophysical Journal, 81*(2), 685-696. doi: https://doi.org/10.1016/S0006-3495(01)75733-5

Coccimiglio, M. L., & Jonz, M. G. (2012). Serotenergic neuroepithelial cells of the skin in developing zebrafish: morphology, innervation and oxygen-sensitive properties. *The Journal of Experimental Biology, 215*, 3881-3894. doi: doi:10.1242/jeb.074575

Conley, D. J., Carstensen, J., Aigars, J., Axe, P., Bonsdorff, E., Eremina, T., . . . Zillén, L. (2011). Hypoxia Is Increasing in the Coastal Zone of the Baltic Sea. *Environmental Science & Technology, 45*(16), 6777-6783. doi: 10.1021/es201212r

Dalla Via, J., Thillart, G. v. d., Cattani, O., & Zwaan, A. d. (1994). Influence of long-term hypoxia exposure on the energy metabolism of *Solea solea* II. Intermediary metabolism in blood, liver and muscle. *Marine Ecology Progress Series, 111*, 17-27.

Dean, B. W., Rashid, T. J., & Jonz, M. G. (2017). Mitogenic Action of Hypoxia upon Cutaneous Neuroepithelial Cells in Developing Zebrafish. *Developmental Neurobiology*, 789-801. doi: DOI 10.1002/dneu.22471

Dejours, P. (1981). *Principles of comparative respiratory physiology*: sole distributors for the USA and Canada, Elsevier North-Holland.

Diaz, R. J., & Breitburg, D. L. (2009). Chapter 1 The Hypoxic Environment. In J. G. Richards, A. P. Farrell, & C. J. Brauner (Eds.), *Fish Physiology* (Vol. 27, pp. 1-23): Academic Press.

Driver, S. E., Robinson, G. S., Fanagan, J., Shen, W., Smith, L. E., Thomas, D. W., & Roberts, P. C. (1999). Oligonucleotide-based inhibition of embryonic gene expression. *Nature Biotechnology, 17*, 1184-1187.

Eisen, J., & Smith, J. (2008). Controlling morpholio experiments: don't stop making antisense. *Development, 135*, 1735-1743.

Engeszer, R., Patterson, L., Rao, A., & Parichy, D. (2007). Zebrafish in the Wild: A Reveiw of Natural History and New Notes from the Field. *Zebrafish, 4*(1), 21-36. doi: 10.1089/zeb.2006.9997

Ferrell, R., & Himmelblau, D. (1967). Diffusion Coefficients of Nitrogen and Oxygen in Water. *Journal of chemical and engineering data, 12*(1).

Gilmour, K. M., & Perry, S. F. (2009). Carbonic anhydrase and acid–base regulation in fish. *Journal of Experimental Biology, 212*(11), 1647.

Gilmour, K. M., Thomas, K., Esbaugh, A. J., & Perry, S. F. (2009). Carbonic anhydrase expression and CO2 excretion during early development in zebrafish Danio rerio. *J Exp Biol, 212*(Pt 23), 3837-3845. doi: 10.1242/jeb.034116

Grossmann, U. (1982). Simulation of combined transfer of oxygen and heat through the skin using a capillary-loop model. *Mathimatical Biosciences, 61*, 205-236.

Habeck, H., Odenthal, J., Walderich, B., Maischein, H.-M., Screen Consortium, T., & Stefan, S.-M. (2002). Analysis of a Zebrafish VEGF Receptor Mutant Reveals Specific Disruption of Angiogenesis. *Current Biology, 12*, 1405-1412.

Henriksson, P., Mandic, M., & Richards, Jeffrey G. (2008). The Osmorespiratory Compromise in Sculpins: Impaired Gas Exchange Is Associated with Freshwater Tolerance. *Physiological and Biochemical Zoology, 81*(3), 310-319. doi: 10.1086/587092

Hierck, B. P., Van Der Heiden, K., Poelma, C., Westerwel, J., & Poelmann, R. E. (2008). Fluid Shear Stress and Inner Curvature Remodeling of the Embryonic Heart. Choosing the Right Lane! *The Scientific World Journal, 8*, 212-222. doi: http://dx.doi.org/10.1100/tsw.2008.42

Hochachka, P. W. (1986). Defense Stategies Against Hypoxia and Hypothermia. *Science, 231*, 234-241.

Hochachka, P. W., & Lutz, P. L. (2001). Mechanism, origin, and evolution of anoxia tolerance in animals. *Comp Biochem Physiol B, 130*, 435-459.

Holeton, G. F. (1970). Oxygen uptake and circulation by a hemoglobinless antarctic fish (Chaenocephalus aceratus Lonnberg) compared with three red-blooded antartic fish. *Comparative Biochemistry and Physiology, 34*(2), 457-471. doi: https://doi.org/10.1016/0010-406X(70)90185-4

Iyer, N. V., Kotch, L. E., Agani, F., Leung, S. W., Laughner, E., Wenger, R. H., . . . Semenza, G. L. (1997). Cellular and developmental control of O2 homeostasis by hypoxia-inducible factor 1α. *Genes & Development, 12*, 149-162.

Jacob, E., Drexel, M., Schwerte, T., & Pelster, B. (2002). Influence of hypoxia and hypoxemia on the development of cardiac activity in zebrafish larvae. *American Journal of Physiology*

doi: 10.1152/ajpregu.00673.2001

Jonz, M. G., Fearon, I. M., & Nurse, C. A. (2004). Neuroepithelial oxygen chemoreceptors of the zebrafish gill. *J Physiol, 560*(3), 737-752. doi: 10.1113/jphysiol.2004.069294

Jonz, M. G., & Nurse, C. A. (2003). Neuroepithelial Cells and Associated Innervation of the Zebrafish Gill: A Confocal Immunoflourescence Study. *The Journal of Comparative Neurology, 461*, 1-17.

Jonz, M. G., & Nurse, C. A. (2005). Development of oxygen sensing in the gills of zebrafish. *The Journal of Experimental Biology, 208*(Pt 8), 1537-1549. doi: 10.1242/jeb.01564

Jonz, M. G., & Nurse, C. A. (2006). Ontogenesis of oxygen chemoreception in aquatic vertebrates. *Respir Physiol Neurobiol, 154*, 139-152.

Jonz, M. G., Zachar, P. C., Da Fonte, D. F., & Mierzwa, A. S. (2015). Peripheral chemoreceptors in fish: A brief history and a look ahead. *Comp Biochem Physiol A Mol Integr Physiol, 186*, 27-38. doi: 10.1016/j.cbpa.2014.09.002

Kajimura, S., Aida, K., & Duan, C. (2005). Insulin-like growth factor-binding protein-1 (IGFBP-1) mediates hypoxia-induced embryonic growth and developmental retardation. *Proceedings of the National Academy of Sciences of the United States of America, 102*(4), 1240.

Kajimura, S., Aida, K., & Duan, C. (2006). Understanding Hypoxia-Induced Gene Expression in Early Development: In Vitro and In Vivo Analysis of Hypoxia-Inducible Factor 1-Regulated Zebra Fish Insulin-Like Growth Factor Binding Protein 1 Gene Expression. *Molecular and Cellular Biology, 26*(3), 1142-1155. doi: doi:10.1128/MCB.26.3.1142-1155.2006

Kamei, H., Lu, L., Jiao, S., Li, Y., Gyrup, C., Laursen, L., . . . Duan, C. (2008). Duplication and Diversification of the Hypoxia-Inducible IGFBP-1 Gene in Zebrafish. *PLoS One, 3*(8), E3091. doi: https://doi.org/10.1371/journal.pone.0003091

Kimmel, C., Ballard, W., Kimmel, S., Ullmann, B., & Schilling, T. (1995). Stages of Embryonic Development of the Zebrafish. *Developmental Dynamics, 203*, 253-310.

Kleiber, M. (1961). *The fire of life. An introduction to animal energetics*: John Wiley & Sons, Inc., New York: London.

Krogh, A. (1941). *The Comparative Physiology of Respiratory Mechanisms*. London, Great Britain: Oxford University Press.

Kuhn, W., Ramel, A., Kuhn, H., & Marti, E. (1963). The filling mechanism of the swimbladder. *Experientia, 19*(10), 497-511. doi: 10.1007/BF02150881

Kumai, Y., Bahubeshi, A., Steele, S., & Perry, S. F. (2011). Strategies for maintaining Na+ balance in zebrafish (*Danio rerio*) during prolonged exposure to acidic water. *Comparative Biochemistry and Physiology, 160*(1), 52-62. doi: 10.1016/j.cbpa.2011.05.001

Lappivaara, J., Nikinmaa, M., & Tuurala, H. (1995). Arterial oxygen tension and the structure of the secondary lamellae of the gills in rainbow trout (Oncorhynchus mykiss) after acute exposure to zinc and during recovery. *Aquatic Toxicology, 32*(4), 321-331. doi: https://doi.org/10.1016/0166-445X(94)00097-A

Larimer, J. L. (1959). Hemoglobin Concentration and Oyxgen Capacity of Mamalian Blood. *Journal of The Elisha Mitchell Scientific Society, 75*(2), 174-177.

Lawrence, C. (2007). The husbandry of zebrafish (*Danio rerio*): A reveiw. *Aquaculture, 269*, 1-20.

Leino, R. L., & McCormick, J. H. (1993). Responses of juvenile largemouth bass to different pH and aluminum levels at overwintering temperatures: effects on gill morphology, electrolyte balance, scale calcium, liver glycogen, and depot fat. *Canadian Journal of Zoology, 71*(3), 531-543. doi: 10.1139/z93-074

Liu, Y. W., & Chan, W. K. (2002). Thyroid hormones are important for embryonic to larval transitory phase in zebrafish. *Differentiation, 70*(1), 36-45. doi: doi:10.1046/j.1432-0436.2002.700104.x

Maron, B. J., Shirani, J., Poliac, L., Mathenage, R., Roberts, W., & Mueller, F. O. (1996). Sudden Death in Young Competitive Atheletes *JAMA, 276*(3), 199-204.

Matear, R. J., & Hirst, A. C. (2003). Long-term changes in dissolved oxygen concentrations in the ocean caused by protracted global warming. *Global Biogeochemical Cycles, 17*(4). doi: 10.1029/2002GB001997

McCormick, J. H., Jensen, K. M., & Leino, R. L. (1989). Survival, Blood Osmolality, and Gill Morphology of Juvenile Yellow Perch, Rock Bass, Black Crappie, and Largemouth Bass Exposed to Acidified Soft Water. *Transactions of the American Fisheries Society, 118*(4), 386-399. doi: 10.1577/1548-8659(1989)118<0386:SBOAGM>2.3.CO;2

Moore, F. B.-G., Hosey, M., & Bagatto, B. (2006). Cardiovascular system in larval zebrafish responds to developmental hypoxia in a family specific manner. *Frontiers in Zoology, 3*(4). doi: doi:10.1186/1742-9994-3-4

Moriyama, S., Ayson, F. G., & Kawauchi, H. (2000). Growth Regulation by Insulin-like Growth Factor-I in Fish. *Bioscience, Biotechnology, and Biochemistry, 64*(8), 1553-1562. doi: 10.1271/bbb.64.1553

Naqvi, S. W. A., Jayakumar, D. A., Narvekar, P. V., Naik, H., Sarma, V. V. S. S., D'Souza, W., . . . George, M. D. (2000). Increased marine production of N2O due to intensifying anoxia on the Indian continental shelf. *Nature, 408*, 346. doi: 10.1038/35042551

https://www.nature.com/articles/35042551#supplementary-information

Nasevicius, A., Larson, J., & Ekker, C. S. (2000). Distinct requirements for zebrafish angiogenesis revealed by a VEGF-A morphant. *Yeast, 17*, 294-301.

Newton, H. (1928). The Oxygen Consumption of Luminous Bacteria. *The Journal of General Physiology, 20*(5), 469 - 475.

Nguyen, C. T., Lu, Q., Wang, Y., & Chen, J. N. (2008). Zebrafish as a model for cardiovascular development and disease. *Drug Discovery Today: Disease models, 5*(3), 135-140. doi: http://doi.org/10.1016/j.ddmod.2009.02.003

Nurse, C. A., & Vollmer, C. (1997). Role of Basic FGF and Oxygen Control of Proliferation, Survival, and Neuronal Differentiation in Carotid Body Chromaffin Cells. *Developmental Biology, 184*, 197-206.

Nusslein-Volard, C., & Dahm, R. (2002). *Zebrafish: a practical approach* New York: Oxford University Press.

Pardal, R., Ortega-Saenz, P., Duran, R., & Lopez-Barneo, J. (2007). Glia-like Stem Cells Sustain Physiologic Neurogensis in the Adult Mammalian Carotid Body. *Cell, 121*, 364-377. doi: DOI 10.1016/j.cell.2007.07.043

Pelster, B., & Burggren, W. W. (1996). Disruption of Hemoglobin Oxygen Transport Does Not Impact Oxygen-Dependent Physiological Processes in Developing Embryos of Zebra Fish (*Danio rerio*). *Circulation Research, 79*(2), 358-362.

Pelster, B., & Scheid, P. (1992). Countercurrent Concentration and Gas Secretion in the Fish Swim Bladder. *Physiological Zoology, 65*(1), 1-16. doi: 10.1086/physzool.65.1.30158236

Perry, S. F., & Gilmour, K. M. (2010). Oxygen uptake and transport in water breathers. In G. E. Nilsson (Ed.), *Respiratory Physiology of Vertebrates: Life With and Without Oxygen* (pp. 49-94). Cambridge: Cambridge University Press.

Perry, S. F., Jonz, M. G., & Gilmour, K. M. (2009). Chapter 5 Oxygen Sensing And The Hypoxic Ventilatory Response. *27*, 193-253. doi: 10.1016/s1546-5098(08)00005-8

Perry, S. F., & Tzaneva, V. (2016). The sensing of respiratory gases in fish: Mechanisms and signalling pathways. *Respir Physiol Neurobiol, 224*, 71-79. doi: https://doi.org/10.1016/j.resp.2015.06.007

Pitman, R. (2011). Regulation of Tissue Oxygenation. In S. Rafael (Ed.): Morgan & Claypool Life Sciences.

Platero-Luengo, A., Gonzalez-Granero, S., Duran, R., Diaz-Castro, B., Piruat, J., Garcia-Verdugo, J. M., . . . Lopez-Barneo, J. (2014). An O_2-Sensitive GLomus Cell-Stem Cell Synapse Induces Crotid Body Growth in Chronic Hypoxia. *Cell, 156*, 291-303. doi: http://dx.doi.org/10.1016/j.cell.2013.12.013

Randall, D. (1982). The control of respiration and circulation in fish during exercise and hypoxia. *The Journal of Experimental Biology, 100*, 275-288.

Rich, P. (2003). The molecular machinery of Keilin's respiratory chain. *Biochemical Society Transactions, 31*(6), 1095-1105. doi: 0.1042/bst0311095

Richard, T. (1996a). Calculating the Oxygen Diffusion Coefficient in Air. Retrieved Jan 8, 2018, 2018, from http://compost.css.cornell.edu/oxygen/oxygen.diff.air.html

Richard, T. (1996b). Calculating the Oxygen Diffusion Coefficient in Water. Retrieved Jan 8, 2018, 2018, from http://compost.css.cornell.edu/oxygen/oxygen.diff.water.html

Robertson, A. B. (2017). *Fluorescent implantable elastomer tags for the measurement of oxygen in insects.* (Text). Retrieved from https://open.library.ubc.ca/collections/24/items/1.0349031

Robertson, C. E., Wright, P. A., Koblitz, L., & Bemier, N. J. (2014). Hypoxia-inducible factor-1 mediates adaptive developmental plasticity of hypoxia tolerance in zebrafish, *Danio rerio*. *Proceedings Of The Royal Society B, 281*. doi: DOI: 10.1098/rspb.2014.0637

Rombough, P. J. (1998). Partitioning Of Oyxgen Uptake Between The Gills And Skin In Fish Larvae: A Novel Method For Estimating Cutaneous Oxygen Uptake. *Journal of Experimental Biology, 201*, 1763-1769.

Rombough, P. J. (2002). Gills are needed for ionoregulation before they are needed for I2 uptake in developing sebrafish, *Danio rerio*. *The Journal of Experimental Biology, 205*, 1787-1794.

Rombough, P. J., & Drader, H. (2009). Hemoglobin enhances oxygen uptake in larval zebrafish (Danio rerio) but only under conditions of extreme hypoxia. *The Journal of Experimental Biology, 212*, 778-784. doi: 10.1242/jeb.026575

Rombough, P. J., & Moroz, B. M. (1997). The Scaling and Potential Importance of Cutaneous and Branchial Surfaces in Respiratory Gas Exchange In Larval and Juvenile Walleye *Stizostedion Vitreum*. *The Journal of Experimental Biology, 200*, 2459-2468.

Schaefer, J., & Ryan, A. (2006). Developmental plasticity in the thermal tolerance of zebrafish Danio rerio. *J Fish Biol, 69*(3), 722-734. doi: 10.1111/j.1095-8649.2006.01145.x

Schwerte, T., Prem, C., Mairosl, A., & Pelster, B. (2006). Development of the sympatho-vagal balance in the cardiovascular system in zebrafish (*Danio rerio*) characterized by power spectrum and classical signal analysis. *The Journal of Experimental Biology, 209*, 1093-1100. doi: doi:10.1242/jeb.02117

Schwerte, T., Uberbacher, D., & Pelster, B. (2003). Non-invasive imaging of blood cell concentration and blood distribution in zebrafish *Danio rerio* incubated in hypoixc conditions *in vivo*. *The Journal of Experimental Biology, 206*, 1299-1307. doi: doi:10.1242/jeb.00249

Sehnert, A. J., Huq, A., Weinstein, B. M., Walker, C., Fishman, M., & Stainier, D. Y. (2002). Cardiac troponin T is essential in sarcomere assembly and cardiac contractility. *Nat Genet, 31*(1), 106-110. doi: 10.1038/ng875

Sollid, J., & Nilsson, G. E. (2006). Plasticity of respiratory structures — Adaptive remodeling of fish gills induced by ambient oxygen and temperature. *Respir Physiol Neurobiol, 154*(1), 241-251. doi: https://doi.org/10.1016/j.resp.2006.02.006

Steele, S., Hong Andy Lo, K., Wai Tsun Li, V., Han Cheng, S., Ekker, M., & Perry, S. F. (2009). Loss of M2 muscarinic receptor function inhibits development of hypoxic bradycardia and alters cardiac !-adrenergic sensitivity in larval zebrafish (Danio rerio). *Am J Physiol Regul Integr Comp Physiol, 297*, R412-R420. doi: doi:10.1152/ajpregu.00036.2009

Subczynski, W. K., Hyde, J. S., & Kusumi, A. (1989). Oxygen Permeability of Phosphatidylcholine-Cholesterol Membranes. *Proc. Natl. Acad. Sci. Biophysics, 86*, 4474-4478.

Thierfeider, L., Watkins, H., MacRae, C., Lamas, R., McKenna, W., Vosberg, H.-P., . . . Seidman, C. E. (1994). Alpha-Tropomysoin and Cardiac Troponin T Mutations Cause Familial Hypertrophic Cardiomyopathy: A disease of the Sarcomere. *Cell, 77*, 701-712.

Ton, C., Stamatiou, D., & Liew, C.-C. (2003). Gene expression profile of zebrafish exposed to hypoxia during development. *Physiology Genomics, 13*, 97-106.

Tuurala, H., Egginton, S., & Soivio, A. (2005). Cold exposure increases branchial water–blood barrier thickness in the eel. *J Fish Biol, 53*(2), 451-455. doi: 10.1111/j.1095-8649.1998.tb00993.x

van Raaij, M. T. M., Pit, D. S. S., Balm, P. H. M., Steffens, A. B., & van den Thillart, G. E. E. J. M. (1996). Behavioral Strategy and the Physiological Stress Response in Rainbow Trout Exposed to Severe Hypoxia. *Hormones and Behavior, 30*(1), 85-92. doi: https://doi.org/10.1006/hbeh.1996.0012

Weibel, E. R. (1984). *The Pathway for Oxygen. Struture and Function in the Mamalian Respiratory System*. Cambridge, Massachusetts and London: Harvard University Press.

Wells, P. R., & Pinder, A. W. (1996). The Respiratory Development of Atlantic Salmon II. Partitioning of Oxygen Uptake Among Gills, Yolk Sac and Body Surfaces. *The Journal of Experimental Biology, 199*, 2737-2744.

Westerfield, M., Howe, D., & Eagle, A. (2015). ZFIN Anatomical Structures by Developmental Stage. Retrieved 01/08, 2016, from http://zfin.org/action/ontology/show-anatomy-terms-by-stage?stage.zdbID=ZDB-STAGE-010723-16

Winata, C., Korzh, S., Kondrychyn, I., Zheng, W., Korzh, V., & Gong, Z. (2009). Development of zebrafish swimbladder: The requirement of Hedgehog signaling in specification and organization of the three tissue layers. *Developmental Biology, 331*, 222-236.

Wood, A. W., Duan, C., & Bern, H. A. (2005). Insulin-Like Growth Factor Signaling in Fish *International Review of Cytology* (Vol. 243, pp. 215-285): Academic Press.

Wood, C., & Shelton, G. (1980). The reflex control of heart rate and cardiac output in the rainbow trout: Interactive influences of hypoxia, haemorrhage, and systemic vasomotor tone. *The Journal of Experimental Biology, 87*, 271-284.

Zhu, Y., Song, D., Tran, N.-T., & Nguyen, N. (2007). The effects of the members of growth hormone family knockdown in zebrafish development. *General and Comparative Endocrinology, 150*(3), 395-404. doi: https://doi.org/10.1016/j.ygcen.2006.10.009